Carbon Nanomaterials for Wastewater Treatment

Hanna S. Abbo[1,2], K. C. Gupta[3],*, Nader G. Khaligh[4], Salam J. J. Titinchi[1],*

Abstract

The research progress made in recent years in removal of organic-inorganic pollutants from wastewater using various types of carbon materials as adsorbents such as carbon nanotubes, carbon nanofibers, graphenes, graphitic carbon nitride, fullerene, activated carbon spheres, and carbon quantum dots is reviewed. These carbon nanomaterials with hierarchical structures are efficient and economical adsorbents. The techniques of metal impregnation and doping help to control the porosity and surface area of nanomaterials. Electrostatic forces, π-π and π-e interactions, van der Waals weak forces, and oxygen-containing groups are considered responsible for the removal of pollutants from wastewater. The carbon nanomaterial-based photocatalysts are applied successfully in decomposition of persistent dyes under visible light. Fe_3O_4 magnetic material is employed as recyclable adsorbent after treatment of wastewater. Freundlich and Langmuir models are found more suitable to calculate the adsorption efficiency and adsorption kinetics of pollutants. Criteria and properties of carbon nanomaterials are discussed that might play a significant role in remediation of wastewater.

Keywords: Adsorption, Carbon nanomaterials, Decomposition, Organic-inorganic pollutants, Wastewater treatment

Received: January 18, 2021; *revised:* March 27, 2021; *accepted:* May 17, 2021

DOI: 10.1002/cben.202100003

1 Introduction

The growing menace of environmental pollution is a subject of great concern as it is causing irreversible damage to human lives across the globe. The primary sources of organic, inorganic, and biological pollutants to terrestrial and aquatic bodies are industrial effluents, anthropogenic emissions, and domestic discharges. Water is an important necessity for the survival of human lives on this earth as only 1 % of the total water is available worth drinking from rivers, lakes, and reservoirs. The scarcity of fresh water is often attributed due to its contamination by industrial effluents, colonial growth of microbes, and pathogens.

Ground and surface water is usually contaminated with heavy metal pollutants that are released by vehicles, industries, and by the seepage of acid mine drainage (AMD) systems. The shortage of drinking water supplies is directly related to waterborne diseases and poverty. For the sustenance of life on earth, water should be preserved both globally and locally. Unlike biodegradable organic pollutants, heavy metal pollutants remain persistent in water and need to be separated. The release of heavy metal pollutants as a secondary by-product of emissions into air, water, and soil is often a threat to human lives and ecological systems. Thus, recovery and preservation of fresh water is a matter of great concern due to increased population, industrialization, urbanization, and variations in climatic parameters [1].

Traditionally, the treatment of wastewater is performed by three main processes, i.e., primary, secondary, and tertiary processes. The primary treatment process involves the separation of suspended solids from wastewater. The secondary treatment process refers to the removal of biodegradable compounds, and in the tertiary treatment process the non-biodegradable compounds are eliminated from the wastewater. To produce safe drinking water, numerous water treatment techniques are commonly applied to remove the pollutants from domestic and industrial wastewater [2]. To follow the regulations to reduce liquid waste discharge and to reduce the

[1] Prof. Hanna S. Abbo, Prof. Salam J. J. Titinchi
Department of Chemistry, University of the Western Cape, Cape Town, South Africa.
E-Mail: stitinchi@uwc.ac.za

[2] Prof. Hanna S. Abbo
Department of Chemistry, University of Basrah, Basrah, Iraq.

[3] Prof. K. C. Gupta
Polymer Research Laboratory, Department of Chemistry, Indian Institute of Technology, Roorkee, 247 667, India.
E-Mail: kcgupta@cy.iitr.ac.in; kcgptfcy@iitr.ac.in

[4] Dr. Nader G. Khaligh
Nanotechnology and Catalysis Research Center, Institute of Postgraduate Studies, University of Malaya, Kuala Lumpur, Malaysia.

cost of the products, most of the industries now have installed wastewater treatment plants for the recovery of water for reuse applications. In these plants, physicochemical methods including chemical precipitation and biological treatment methods are commonly employed. However, these methods are quite effective in reducing the load of organic pollutants to a permissible limit but often fail in reducing the load of heavy metal pollutants to a permissible limit.

To eliminate the organic pollutants from wastewater, conventional techniques such as biological processes, activated carbon (AC) adsorption, ozonization, photocatalysis, and wetlands treatment methods are commonly used. But these conventional methods are also associated with their own shortcomings of inefficiency and cost effectiveness.

The chemical precipitation process is cost-effective but produces large amounts of sludge and secondary waste that contribute an additional cost to this process. Conventionally, the chemical precipitation process is carried out by precipitating metal pollutants as hydroxides or sulfides [3] despite of accumulation of a large amount of metal hydroxide sludge in nature. Besides this, it also needs an additional separation step for the flocculation and sedimentation of resultant precipitates. Further, the removal of heavy metal ions from wastewater is not limited only to physicochemical methods but also other separation techniques are suitable. The physicochemical methods have drawbacks in terms of generating products mostly in impure forms due to being nonselective in their nature. On the other hand, the selective separation techniques such as ion exchange, membrane filtration, solvent extraction, and adsorption methods [4, 5] have become more useful as they are able to yield products in purified forms. The technique of solvent extraction in wastewater purifications is well established and was initially applied by various industries for separation of uranium and copper. But the adsorption process is found to be more economical and a viable approach in simultaneous removal of multiple pollutants using a wide range of adsorbents.

Generally, adsorption is a dynamic equilibrium process involving the attachment of adsorbates on a solid surface or to an interface through van der Waals forces of attraction [6] or electrostatic interactions [7]. In the adsorption process, the attachment of adsorbates to a surface or interface takes place either through physisorption or chemisorption processes. Owing to a wide range of van der Waals weak forces of attractions between adsorbates and adsorbents, physisorption is found to be nonspecific in nature.

So far, various type of adsorbents are in use for the treatment of wastewater such as carbon nanotubes [8–10], graphenes and its derivatives [11], natural zeolites, and modified organic wastes [12]. Currently, the interest in using chemically modified organic wastes as adsorbents for the treatment of wastewater has increased due to their cost effectiveness and biodegradability. The technique of modification of agricultural-based organic substrates is simple and straightforward. However, the modified organic substrates are nonselective and have low affinity for targeted metal pollutants, and at the same time they cause a significant decrease in the oxygen content of wastewater prior to the separation of targeted heavy metal pollutants. Thus, as a result of reduction the in oxygen content in wastewater, the survival of aquatic life becomes a great challenge. Various types of adsorbents are employed in the removal of heavy metal ions from wastewater but most of these need an additional step for their recoveries after completion of the adsorption process. Sometimes these adsorbents also have limitations of their regeneration and need a longer processing time. Thus, there is a need to have a material or technique that would overcome these limitations of macro-sized natural adsorbents used in the treatment of wastewater and which are able to fulfil the ever growing demand of fresh water for various applications.

The application of nanotechnology and nanomaterials is a scientific choice to overcome these limitations of conventional macro-sized adsorbents that are commonly used in wastewater treatment. Nano-sized adsorbents [13] are comparatively more efficient in overcoming inherent limitations of macro-sized adsorbents; hence, the application of nanotechnology has become an effective way for the treatment of wastewater. Recently, nano-sized photocatalysts have received great attention in the area of wastewater treatment [14] due to their exceptionally high photocatalytic activity in decomposition of organic pollutants using visible sunlight [15]. Thus, the development of an efficient technique for the separation of heavy metal ions and decomposition of organic water pollutants is a topic for current research since the past two decades. Amongst the various sources of pollutants, the textile and printing industries are the main sources of organic pollutants that are releasing approximately 15 % of the world production of dyes as effluents. The textile dyes, organic pollutants, and other commercial colorants are usually persistent; hence, they need special attention to ensure their degradation in wastewater to overcome the scarcity of fresh water.

In view of the various problems of water pollutants and limitations of existing methods, there is a need for careful planning to carry out focused research to develop remedial and effective methods for the removal of pollutants from wastewater, which are discharged by various industries and causing adverse effects on human health and ecosystems. Amongst the different types of adsorbents used in remediation of water pollutants, carbonaceous nanomaterial is found to be quite suitable for the removal of organic dyes and heavy metal ions pollutants from industrial wastewater. This review highlights the potential of various types of carbon nanomaterials that have been used frequently in the treatment of wastewater during the last one decade.

2 Carbon Nanomaterials for Water Treatment

The discovery of C60 has opened a new branch of carbon chemistry, covering various types of carbon nanostructures such as graphenes (2D), carbon nanotubes (1D), carbon quantum dots, carbon nanofibers (CNFs), fullerenes (0D), nanoporous carbons (NPCs), and activated carbon spheres (ACS). Currently, these carbon nanostructures are also being used in different applications ranging from storage of solar energy [16, 17] to the fabrication of sensing devices [18]. Various carbon nanostructures such as carbon nanotubes (CNTs), graphenes (G), activated carbons (ACs), and activated carbon

spheres (ACSs) are found potentially useful in remediation of wastewater problems as efficient adsorbents as discussed in the following sections of this review.

2.1 Carbon Nanotubes and Carbon Nanofibers

2.1.1 Carbon Nanotubes

CNTs are one-dimensional nanomaterials, which have perfectly hexagonally connected carbon atoms with distinct thermal, electrical, and mechanical properties. CNTs exist either as single-walled CNTs (SWCNTs) or multi-walled CNTs (MWCNTs) with concentric seamless graphene cylinders having an adjacent spacing of about 0.34 nm (Fig. 1). CNTs are hard and stronger than any other known material due to the presence of sp^2 type carbon atoms to join through covalent bonding. The oxygen-containing functional groups are easily introduced at the surface of CNTs by chemical modification and also removed easily by heating. The adsorption of pollutants on CNTs is attributed to π-π interactions, hydrophobic interactions, electrostatic and charge transfer interactions. The compatible pore size and hexagonally arranged carbon atoms in CNTs provide strong and favorable interactions between CNTs and pollutants. In addition to various properties of CNTs, the geometry of organic pollutants also influences the extent of adsorption at the surface of CNTs, i.e., pollutant molecules with planar structures are adsorbed stronger than those with non-planar structures.((Figure 1))

CNTs have been used widely in removal of heavy metal ions [19–22] and organic dyes [23–25] from water due to their excellent physical and chemical properties such as: small size, high surface-to-volume ratio, low density, high porosity, hollow structures, controllable pore size distribution, large surface area, chemical inertness, high mechanical strength, electrical conductivity, and outstanding water-transport property. Due to high porosity and high surface-to-volume ratio, CNTs have revealed an exceptionally high sorption capacity [26] as compared to conventional granular and powdered activated carbon (AC) [24]. The CNTs as nanoporous adsorbents are also used effectively in removal of various biological contaminants and to enhance the photocatalytic activities of TiO_2 semiconductors by controlling charge separation [27]. CNTs in combination with TiO_2 are able to enhance the decomposition of organic pollutants in the presence of UV light radiation.

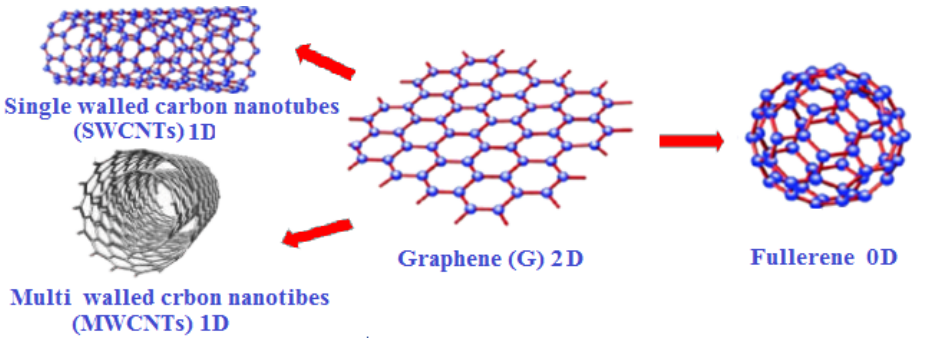

Figure 1. Carbon nanomaterials used in treatment of wastewater.

The adsorptive capacity and selectivity of CNTs for organic dyes and metal ions from wastewater promoted an increasing trend on creating required functionalities at their surfaces [9, 28, 29]. During the last decade, the attention was also focused to develop CNTs-based nanocomposites for the removal of organic dyes and heavy metal ions pollutants from wastewater [8, 30–32]. CNTs composites were developed for the fabrication of permselective membranes for the desalination of brackish water and treatment of wastewater, i.e., for the separation of heavy metal ions and oil spillage from water [33].

Nanocomposite photocatalysts with noble metals and bimetals (Ag or Pd/TiO_2/CNT) were prepared by using CNTs in a modified dry-mix metal-organic chemical vapor deposition method (MO-CVD), and their photocatalytic activities were evaluated by studying the decomposition of methylene blue (MB) as a model probe reaction [34]. Results indicated that the silver-titania CNT nanocomposites (Ag/TiO_2/CNTs) with 2 % Ag were the most efficient photocatalysts for the decomposition of MB (50 mg L^{-1}) within a period of 4 h (92 %) in the presence of the optimum amount of photocatalyst (1 g L^{-1}). This positive outcome was due to the plasmonic effect of added Ag, which increased the photocatalytic activity of TiO_2/CNTs by about 10 %.

In comparison to Ag, palladium had only a little effect in varying the photocatalytic activity of titania-CNT nanocomposites (TiO_2/CNTs) but in the presence of both metals together (Ag and Pd), the photocatalytic activity of titania-CNT nanocomposites in degradation of MB was reduced significantly [34]. The CNTs modified with polyamidoamine dendrimers (PAMAM, G4) were also used successfully in the elimination of Cu(II) and Pb(II) ions from wastewater having single and binary mixtures of metal ions in solution [35].

Lignin, a naturally occurring polymer, was grafted on CNTs to prepare a 3D nanocomposite for the removal of Pb(II) ions from wastewater [36]. The lignin-grafted 3D nanocomposite exhibited a high adsorption capacity for Pb(II) ions (235 mg L^{-1}) from wastewater, which was due to enhanced surface area, pore size, and more oxygen-containing groups on CNTs in comparison to pristine CNTs. The improved removal efficiency of CNTs at high pH was due to the presence of a large number of oxygen-containing groups, which facilitated the removal of Pb(II) ions through electrostatic attractions. The 3D structure of composites has also helped in the separation of CNTs after adsorption of Pb(II) ions.

The performance of CNTs indicated the dependence on covalent/noncovalent chemical interactions that occur between heavy metal ions and active sites on CNTs such as exohedral, endohedral, and open-end interactions, which are created on functionalized CNTs (Figs. 2a–d).

The physical adsorption on unfunctionalized CNTs possibly takes place at available surface sites on CNTs such as pores, interstitial channels (ICs), and grooves

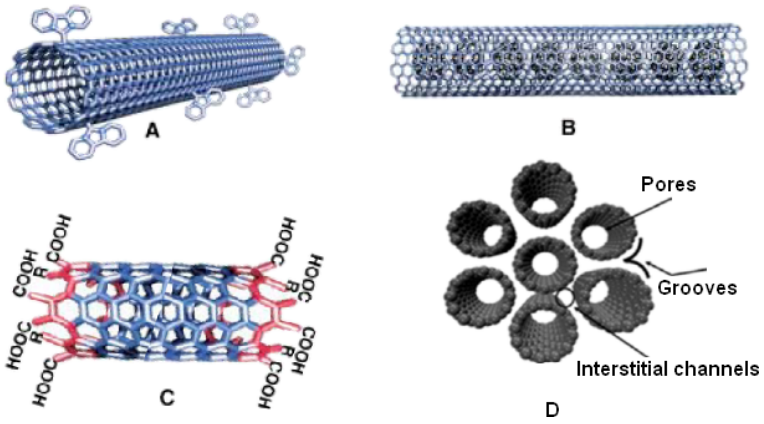

Figure 2. (a) Adsorption sites at the surface of CNTs as side wall/exohedral; (b) inside of CNTs as endohedral; (c) at the open end of CNTs created through covalent/noncovalent functionalization of CNTs; (d) adsorption sites on unfunctionalized CNTs.

(Fig. 2d). The improved removal of various heavy metals ions such as Cd(II), Cr(VI), Pb(II), Ni(II), and Cu(II) ions from wastewater [37] clearly suggested that the adsorptive capacity depends on various parameters of CNTs like surface area, purity, porosity, surface functionalities, active sites density, types of CNTs, and also on the nature of adsorbates.Several reviews on surface-functionalized MWCNTs clearly indicated that these MWCNTs become more selective than pristine or oxidized MWCNTs in removal of organic dyes [9], pharmaceuticals [38], or heavy metal ions from wastewater [9, 29]. The surface-functionalized MWCNTs with 2-aminobenzothiazole, iminodiacetic acid, *L*-cysteine, and chitosan enabled increased and selective removal of metal ions from wastewater [39–41]. Chitosan-modified MWCNTs proved to be useful in removal of anionic pollutants such as phosphate, picric acid, and anionic chromium(VI) due to electrostatic interactions with amino functionality of chitosan and due to the presence of size-selective porosity in removal of anionic pollutants from waste water [42–44]. These studies clearly demonstrated that biopolymers are able to produce MWCNT composites, which have increased functionality and porosity to allow for selective sorption of pollutants from wastewater (Tab. 1).

The technique of metal doping is also employed to improve the adsorption and photodegradation properties of MWCNTs for the treatment of water pollutants. A series of palladium-doped zirconium oxide multiwalled carbon nanotubes nanocomposites (Pd-ZrO_2-MWCNTs) were prepared and tested for their photocatalytic degradation efficiency for acid blue 40 dye in water using simulated sun light [45]. The photocatalytic activity of these nanocomposites loaded with 0.5 % Pd was found to be significantly high (98 %) as compared to ZrO_2 and ZrO_2-MWCNTs photocatalysts within a period of 3 h.

The adsorptive properties of CNTs are due to the presence of various mechanisms such as π-π electron-donor-acceptor (EDA) interactions, electrostatic interactions, hydrogen bonding, and compatible pore size. The EDA interactions are considered as predominant driving force for the removal of organic pollutants or dyes having benzene rings. Considering these attributes of CNTs, it is clear that they are effective adsorbents though expensive. However, the adsorptive properties of CNTs overweigh their cost in comparison to conventional AC, which is both costly and less effective in treatment of wastewater. If CNTs are not considered as an alternative to the wide-spectrum AC, then they cannot be ignored for surface chemistry, which can be tuned to be a contaminant-specific adsorbent in wastewater treatment.

MWCNTs were synthesized by the tubular microwave chemical vapor deposition technique and used successfully for the removal of Cd(II) and Cu(II) ions from wastewater. Various adsorption parameters were investigated. The synthesized MWCNTs exhibited highest adsorption capacities for Cd(II) ions (88.62 mg g^{-1}) than Cu(II) ions (99 mg g^{-1}) within a pH range of 5–5.5 at a dose of 0.1 g within a contact time interval

Table 1. Efficiency of removal of organic/inorganic pollutants from wastewater by different forms of carbonaceous adsorbents.

Adsorbent	Form of adsorbent	Removal of dye/metal ions/oil/organic solvent	Ref.
Carbon nanotubes (CNTs)	CNT sheet	101.05 (Pb^{2+}), 75.84 (Cd^{2+}), 69.63 (Co^{2+},) 58.00 (Zn^{2+}), 50.37 (Cu^{2+}) [mg g^{-1}]	[22]
	MnO_2/CNT	58.8 (Hg^{2+}) [mg g^{-1}]	[31]
	PAMAM-CNT	3333 (Cu^{2+}), 4870 (Pb^{2+}) [mg g^{-1}]	[35]
	L-CNTs, lignin-CNT	235 Pb^{2+} [mg g^{-1}]	[36]
	CNT-NH_2	714 (AB), 666 (ABK) [mg g^{-1}]	[9]
	Gel-CNT-MNPs	96.1 (RD), 76.3% (MB)	[30]
	Ag-TiO_2/CNT	92 % (MB)	[34]
	O_3-treated MWCNT	250 (AAP) [mg g^{-1}]	[38]
	G/CNT beads (HPGCB)	521.5 (MB) [mg mL^{-1}]	[80]

Continued Table 1.

Adsorbent	Form of adsorbent	Removal of dye/metal ions/oil/organic solvent	Ref.
MWCNTs	MWCNT-COOH	143–164 (Cr^{6+}) [mg g^{-1}]	[44]
	Carbazone/MWCNT	14.56 (Pb^{2+}) [mg g^{-1}]	[29]
	CS/MWCNTs	36.10 (PO_4^{3-}) [mg g^{-1}]; 90 % (PA)	[42, 43]
	MWCNT; PAC	409.4 (DB); 135.2 (DB) [mg g^{-1}]	[24]
	ox-MWCNT-PER	257.73 (AZY), 45.39 (AZR) [mg g^{-1}]	[28]
Carbon nanofibers (CNFs)	Fe-CNF	16 As^{5+} [mg g^{-1}]	[58]
	CNFs	567 (MTC), 558 (MO), 493 (AR1) [mg g^{-1}]	[53]
	Fe_3O_4@CNFs	94 % (MB), 75 % (RhB)	[56]
	A-Fe@CNFs	91 % (MB), 83 % (RhB)	[57]
	α-Fe@CNF1100	63 % (MB)	[59]
	CNFs	6.18 (CFN), 4.82 (BP), 0.68 (CP) [mmol g^{-1}]	[62]
Graphene (G)	Sulfonated graphene (GS)	58 (Cd^{2+}) [mg g^{-1}]	[74]
	G-foam(CDGF)	90 (Cr^{6+}) [mg g^{-1}]	[77]
	Graphene/MgO	358.96 (Pb^{2+}), 388.4 (Cd^{2+}), 169.8 (Cu^{2+}) [mg g^{-1}]	[78]
	Graphene	153.85 (MB) [mg g^{-1}]	[71]
	Sulfonated graphene (GS)	400 (Phen), 906 (MB) [mg g^{-1}]	[74]
	Graphene hydrogel GH	308.3 (CFX) [mg g^{-1}]	[75]
	Graphene-CNTs aerogels	100 % (MB), 270 % (MO)	[83]
	3D graphene foams	250 % (OL) and (OS)	[84]
	G nanoplates (CS/GNPs)	230.91 (MO), 132.94 (AR1) [mg g^{-1}]	[86]
	Graphene aerogel (GA)	2.5×10^4 (diesel oil) [mg g^{-1}]	[100]
Graphene oxide (GO)	GO-CS-PVA hydrogels	172.11 (Cd^{2+}), 70.37 (Ni^{2+}) [mg g^{-1}]	[11]
	Few-layered GO (FGO)	1850 (Pb^{2+}) [mg g^{-1}]	[88]
	$NiFe_2O_4$-GO	25.0 (Pb^{2+}), (Cr^{3+}) 5.50 [mg g^{-1}]	[89]
	GOx-microbots	95% (Pb^{2+})	[90]
	GO/cellulose membranes	15.5 (Co^{2+}), 14.3 (Ni^{2+}), 26.6 (Cu^{2+}), 16.7 (Zn^{2+}), 26.8 (Cd^{2+}), 107.9 (Pb^{2+} [mg g^{-1}]	[91]
	GO-Zr-P	363 (Pb^{2+}), 232 (Cd^{2+}), 328 (Cu^{2+}), 251 (Zn^{2+}) [mg g^{-1}]	[92]
	EDTA-mGO	508.4 (Pb^{2+}), 268.4 (Hg^{2+}), 301.2 (Cu^{2+}) [mg g^{-1}]	[94]
	GO-$MnFe_2O_4$	673 (Pb^{2+}), 146 (As^{3+}), 207 (As^{5+}) [mg g^{-1}]	[97]
	GO-PANI	1004 (Pb^{2+}) [mg g^{-1}]	[102]
	GO	294 (Cu^{2+}), 345 (Zn^{2+}), 530 (Cd^{2+}), 1119 (Pb^{2+}) [mg g^{-1}]	[106]
	Graphene oxide	2273 (MB) [mg g^{-1}]	[72]
	GO-PANI	544 (MB) [mg g^{-1}]	[102]
	PVP/PCMC/GO/bentonite	172.14 (MB) [mg g^{-1}]	[103]
	GO-CS	71.6 % (picric acid)	[104]
	GO	135.1 (MB), 66.7 (MO)	[105]

Continued Table 1.

Adsorbent	Form of adsorbent	Removal of dye/metal ions/oil/organic solvent	Ref.
Reduced graphene oxide (rGO)	$ZrO(OH)_{1.33}Cl_{0.66}$–rGO	44.14 (F^-) [mg g^{-1}]	[76]
	rGO-Fe_3O_4	30.68 (Pb^{2+}) [mg g^{-1}]	[108]
	rGO-Co_3O_4	208.8 (Cr^{6+}) [mg g^{-1}]	[109]
	rGO/NiO	198 (Cr^{6+}) [mg g^{-1}]	[110]
	rGO-thymine	128 (Hg^{2+}) [mg g^{-1}]	[111]
	rGO-Mn-TiO_2	97.32 % (Cr^{4+})	[112]
	PDA/rGO/HNT	99.74 % (Cu^{2+}), 99.01 % (Cr^{3+})	[115]
	rGO	476.2 (MG); 144.9 (MB), 243.9 (MO) [mg g^{-1}]	[87, 105]
	MCM-41-rGO	909.1 (aspirin), 555.6 (acetaminophen) [mg g^{-1}]	[98]
	rGO/CTAB	213 (DR80), 79 (DR23) [mg g^{-1}]	[107]
	rGO/PC	17.57 (CCl_4) [g g^{-1}]	[113]
	CFA@$(rGO/TNS)_n$	55.2 % (MB)	[114]
	PDA/rGO/HNT	99.72 % (MB), 99.09 % (CR)	[115]
Graphitic carbon nitrite (g-C_3N_4) (CN)	g-C_3N_4	7.4 Pb^{2+} [mg g^{-1}]	[122]
	C_3N_4/TiO_2-NT	37.1 % MB	[27]
	MCN-1	769 phenol [mg g^{-1}]	[123]
	CN hydrogel	402 (MB) [mg g^{-1}]	[124]
	GN (GO/CNdots)	33.6 % (RhB)	[125]
	O-g-C_3N_4	94.5 % RhB	[126]
	Fe_3O_4-ZnO@g-C_3N_4	95 % (SMX)	[127]
	g-C_3N_4-TiO_2-GA	96.5 % (RhB)	[130]
	Co-g-C_3N_4	97 % (RhB)	[131]
Activated carbons (ACs)	PAC	99.4 % Cr^{6+}	[41]
	PAC	63.3 (Zn^{2+}), 59.8 (Pb^{2+}), 60.9 (Cu^{2+}), 73.6 % (Cd^{2+}) [mg g^{-1}]	[137]
	AC	97–99 % (Ni^{2+}, Co^{2+}, Cd^{2+}, Cu^{2+}, Pb^{2+}, Cr^{3+}), 10 % (Cr^{6+})	[152]
	Thiol-AC	238 (Pb^{2+}), 96 (Cd^{2+}), 88 (Cu^{2+}), 52 Ni^{2+} [mg g^{-1}]	[156]
	Multipore AC (MPAC)	1.34 (Pb^{2+}), 1.07 (Cd^{2+}), 1.22 (Cu^{2+}), 0.97 (Ni^{2+}), 0.93 (Zn^{2+}) [mmol g^{-1}]	[157]
	Ag-AC; Cu-AC	95 % (Br^-, I^-); 4.92 % (NO_3^-)	[160, 164]
	Fe-AC	4.7 As^{3+}, 4, As^{5+}, Hg^{2+} 4.6, 4.4 Pb^{2+} [mg g^{-1}]	[163]
	$CoFe_2O_4$/AC	83.333 (Cr^{6+}) [mg g^{-1}]	[167]
	Fe_2O_3-TiO_2@AC	> 90 % (Cu^{2+} and As^5)	[169]
	CASD-KOH, CASD-$ZnCl_2$	1.0 (Cd^{2+}), 1.6 (Ni^{2+}), 0.2 (Cd^{2+}), 0.3 (Ni^{2+}) [mmol g^{-1}]	[174]
	AC	0.062 (paracetamol) [mg g^{-1}]	[138]
	Fe-AC	357.1 (MB) [mg g^{-1}]	[151]
	$La_{0.6}Nd_{0.4}FeO_3$@AC	99.81 % (MO)	[165]
	$CoFe_2O_4$/NOAC	95 % (AV49)	[166]
	TiO_2/AC	93.2 % (RhB)	[170]
	TiO_2/AC and TiO_2/NC	98.80 %, 95.11 % (MeG)	[171]

Continued Table 1.

Adsorbent	Form of adsorbent	Removal of dye/metal ions/oil/organic solvent	Ref.
Fullerene (F)	Modified fullerene	70 (I^-), 125 (Cu^{2+}) [mg g^{-1}]	[181]
	Polystyrene/fullerene	14.6 (Cu^{2+}) [mmol g^{-1}]	[182]
	Modified fullerene	329 (MB) [mg g^{-1}]	[181]
Nanoporous activated carbon spheres (ACSs)	N_2-CS (NCS)	279 (Cr^{6+}) [mg g^{-1}]	[185]
	Carboxyl-rich ACS	380.1 (Pb^{2+}), 100.8 (Cd^{2+}) [mg g^{-1}]	[186]
	N/S-MCMs/Fe_3O_4	74.5 (Hg^{2+}) [mg g^{-1}]	[187]
	K-CS	276.09 (Cd^{2+}) [mg g^{-1}]	[189]
	ACS	227.7 (Cr^{6}) [mg g^{-1}]	[190]
	BGBH-C-K	469 (MB), 418 (MO) [mg g^{-1}]	[178]
	Spherical carbon	236 (toluene) [g L^{-1}]	[184]
	Porous ACS (PCNS)	3152 (MB), 1455 (MG), 1409 (RhB) [mg g^{-1}]	[188]
	K-CS	382.15 (CR) [mg/g]	[189]
Carbon quantum dots (CQDs)	N-CQD	37 % (Cd^{2+}), 75 % (Pb^{2+})	[191]
	Fe_3O_4/N-CQDs	303.03 (Pb^{2+}) [mg g^{-1}]	[197]
	PECQDs/$MnFe_2O_4$	91% (U^{6+}) [mg g^{-1}]	[198]
	CQDs/ZnAl-LDH	12.60 (Cd^{2+}) [mg g^{-1}]	[200]
	N-CQD	30 min (AB, AR), 90 min (E-Y, MB), 0 min (EBT, MO)	[191]
	CQDs/TiO_2	95 min (MB)	[192]
	ZSH@CQDs	70.4 % (RhB)	[193]
	CQDs/NH_2-MIL-125	100 % (RhB)	[194]
	CQDs/$La_2Ti_2O_7$	99 % (RhB)	[195]
	NCDs/$BiVO_4$	100 % (RhB), 90 % (tetracycline)	[196]
	rPET/MWNT/CQD	98 % (MB)	[199]
Clay-carbon	SBE@C	0.114 TCH [mmol g^{-1}]	[33]

Acetaminophen (AAP); Acid Black (ABK), Acid Blue (AB); Acid Red (AR); Acid Violet (AV); Alizarin Blue (AZB); Alizarin Red (AZR); Bisphenol (BP); Cetyltrimethylammonium Bromide (CTAB), Chitosan (CS); Chlorophenol (CP); Ciprofloxacin (CFN); Coal Fly Ash (CFA); Congo Red (CR), Direct Blue 53 Dye (DB); Direct Red (DR); Eosin Y (E-Y); Eriochrome Black T (EBT); Graphene Aerogel (GA); Graphene-like Porous CN Structure (BGBH); Graphene Nanoplates (GNP), Halloysite Nanotubes (HNTs); Highly Porous G/CNTs beads (HPGCB); Impregnated AC (CASD); Layered Double Hydroxide (LDH); Malachite Green (MG); Mesoporous Carbon Microspheres (MCMs); Mesoporous Carbon Nitride (MCN); Methyl Green (MeG); Methyl Orange (MO); Methyl Thionine Chloride (MTC); Methylene Blue (MB); Natural Clay (NC); Oil (OL); Organic Solvent (OS); Phenanthrene (Phn); Polyamidoamine Dendrimer (PAMAM); Polyaniline (PANI); Polycarbonate (PC); Polydopamine (PDA); Powered Activated Carbon (PAC); Spent Bleaching Earth (SBE); recycled Poly(ethylene terephthalate) (rPET); Red Dye (RD); Rhodamine B (RhB); Sulfamethoxazole (SMX); Tetracycline HCl (TCH).

of 35–50 min with an initial concentration of metal ions of 10 mg L^{-1} [46].

A cost-effective and promising alternative to nanobiocomposite membranes for the removal of dye from wastewater was designed by covalent binding of Jicama peroxidase (JP) at the surface of MWCNTs used in buckypaper/polyvinyl alcohol (BP/PVA)-modified membranes. The modified membranes were found effective in degradation of MB dye (64 %) in wastewater without showing any variation in their removal efficiency even after eight reuse applications. Studies indicated that these membranes are able to have a notable impact on the development of effective green and sustainable wastewater treatment technologies [47]. The efficacy of these membranes in removal of MB was confirmed by applying an artificial neural network approach coupled with particle swarm optimization (ANN-PSO). The applicability of the approach was valid as it provided a significantly high value of regression coefficient R^2 [48].

2.1.2 Carbon Nanofibers

Carbon nanofibers (CNFs) are a 1D form of carbon nanomaterials having low density and high length-to-diameter ratio. Normally, CNFs have diameters between 3–200 nm and lengths in micrometers. Generally, the solutions of cellulose, polyacrylonitrile, polyvinyl alcohol, poly(vinyl pyrrolidone), phenolic resins, and polybenzimidazole are electrospun to produce nanofibers, which by carbonization and activation produce carbon nanofibers with hierarchical pore structures for multifunctional integration [49]. The presence of high surface area, porosity, and surface sites in CNFs make them suitable for the adsorption of pollutants [50]. The surfaces of carbon nanofibers are functionalized easily through chemical modification to make them selective adsorbents [51].

Electroactivated carbon nanofibers-peroxydisulfate (E-ACF-PDS) have been used for efficient removal (98.78 %) of a persistent organic pollutant such as carbamazepine (CBZ) in water within 30 min of electrolysis, which is significantly high in comparison to other activated carbon fibers. These results suggested that the E-ACF-PDS process is potentially useful in removal of CBZ from aqueous solution due to concomitant adsorption of contaminants and increased formation of active radicals on ACF.

Incorporated peroxydisulfate (PDS) was able to generate more sulfate radicals at the surface of CNFs which enhanced the degradation of CBZ efficiently [52]. Different types of mesoporous CNFs were electrospun using phenolic resins as precursor. The Pluronic F127 triblock copolymer was used as a template and the amount of tetraethyl orthosilicate (TEOS) was selected as 1, 2, and 3 g, respectively. The prepared C-1, C-2, and C-3 CNFs had surface areas of 1088, 1176, and 1642 m^2g^{-1}, and the pore volume of these CNFs was 0.65, 0.78, and 1.02 cm^3g^{-1}, respectively. These CNFs were applied successfully for the removal of large-sized dye molecules from wastewater [53].

The removal of the cationic dye methylthionine chloride (MC) improved on increasing the solution pH but in the case of anionic dyes (MO and AR1) the maximum removal was observed at low pH. The C-3 CNF exhibited high adsorptive capacity due to the presence of large-sized pores, which facilitated the removal of large-sized dye molecules. In one of the studies of adsorption on CNF, a theoretical model was also developed to correlate the adsorption of Pb(II) ions from industrial wastewater on CNFs [54]. In these studies, the adsorptive capacity of CNFs for Pb(II) ions was predicted to be 166.6 $mg\,g^{-1}$, which was significantly more than found with other adsorbents.

Magnetic CNFs with hierarchical porous structure were also prepared using polybenzoxazine and Fe_3O_4 for wastewater treatment. The inclusion of magnetic Fe_3O_4 facilitated the separation of CNFs after adsorption was complete [55]. The polybenzoxazine precursor-based magnetic porous CNFs (Fe_3O_4@CNF) with hierarchical structures were prepared and used in the removal of MB and RhB dyes from wastewater [56, 57]. The prepared CNFs had an extremely large surface area (1885 m^2g^{-1}) and high pore volume (2.083 cm^3g^{-1}), which enhanced the adsorption of organic dyes, and the presence of magnetic susceptibility in CNFs allowed their separation after adsorption.

In other studies, Fe-metal and Fe nanoparticles filled carbon nanofibers were prepared and used in removal of As(V) ions [58] and other pollutants such as organic dyes and phenols [59]. The Fe@CNFs and nano-Fe@CNFs carbon nanofibers had high adsorptive capacities and were separated easily from water using an external magnet. The electrostatic attraction forces were considered responsible for the removal of As(V) ions from wastewater, and hydrogen bonding and π-π interactions were considered responsible for the elimination of organic pollutants from wastewater.

The adsorption of As(V) ions on Fe-grown CNFs followed the Freundlich model due to the presence of heterogeneous active sites on the surface of these carbon nanofibers. Like other carbon nanomaterials, the specific surface area, pore size, and pore volume in CNFs were enhanced by a chemical activation process in the presence of various chemical agents such as K_2CO_3, Rb_2CO_3, Cs_2CO_3, KOH, Li_2CO_3, Na_2CO_3, and NaOH. The increase in surface area in CNFs had the following order for the studied chemical activating agents: Cs_2CO_3 > Rb_2CO_3 > KOH > NaOH > Na_2CO_3 > Li_2CO_3 [60]. The observed trend was due to the differences in the size of intercalated cations such as Li(I) (0.12 nm), Na(I) (0.19 nm), K(I) (0.26 nm), Rb(I) (0.3 nm), and Cs(I) (0.338 nm). This activation of CNFs not only opened the already closed pores of CNFs but also produced additional new pores. The larger specific surface area and pore volume enhanced the adsorptive properties of CNFs by 2–3-fold for ciprofloxacin, 2-chlorophenol, and bisphenol [61].

As studies on the adsorptive efficiency of CNFs in water treatment are very limited, there is a need to intensify further research on the development of CNFs with heterostructures and porosities for the removal of pollutants from wastewater. The development of eco-friendly and cost-effective CNFs may open new avenues for research in the area of water treatment.

Microwave was applied to synthesize carbon nanotubes (M-CNT) and carbon nanofibers (M-CNF). CNTs were tested for the removal of dibenzothiophene (DBT) from a model diesel fuel (MDF). The removal capacity of DBT by M-CNT and M-CNF was 43 % and 35 %, respectively [62].

2.2 Graphene, its Derivatives, and Graphitic Carbon Nitride

2.2.1 Graphene

Graphene is a two-dimensional carbon nanomaterial having a layer of sp^2-hybridized carbon atoms packed in a benzene ring structure. The electron rich π-system and highly hydrophobic surface make graphene a potential adsorbent in removal of different types of organic pollutants from wastewater. Graphene and its derivatives are less costly and their adsorption capacities are almost comparable to CNTs used as adsorbent. Therefore, during the last decade, graphene and its derivatives have attracted widespread attention to use them as efficient adsorbents for the removal of pollutants from industrial wastewater.

Normally, water pollutants are oils, organic solvents, dyes, metal ions, and drugs, which cause serious damage to human health and ecological balance. To overcome these problems and

to ensure the availability of fresh water, the graphene-based nanomaterials are considered as efficient adsorbents in the removal of pollutants from industrial and domestic wastewater. Amongst the various types of carbon nanomaterials, the 2D graphene (G), graphene oxide (GO), and reduced graphene (rGO) were found to be highly effective in wastewater treatment similarly to CNTs. The outstanding merits of graphene (G) [63–65], graphene oxide (GO) [66, 67], and reduced graphene oxide (rGO) [68, 69] are mainly due to the large surface area, the presence of abundant active sites, and high selectivity (Fig. 3).

Similarly to CNTs, graphene [5, 70] and its derivatives have a high surface-to-weight ratio ($\sim 2600\ m^2g^{-1}$) and high chemical stability, which qualify them to be as potential adsorbent in the elimination of organic [71, 72] and heavy metal ions from industrial effluents and domestic wastewater [71–73].

Liu et al. have reported on the efficient adsorption of MB dye at the surface of graphene nanosheets at pH 10 [71]. The improved dye uptake at high pH ($\sim 99.68\ \%$) was due to the formation of negatively charged GO, which considerably enhanced the electrostatic interactions with the cationic MB dye. Despite of several advantages associated with graphene to act as an adsorbent, it agglomerates and forms graphite due to strong interplanar interactions and stacking. Therefore, surface functionalization of graphene proved to be useful to prevent its agglomeration. The surface functionalization of graphene with cationic (CTAB) or anionic surfactants (sodium dodecyl sulfate, SDS) not only prevented the agglomeration of graphene but also helped in increasing the adsorption of cationic or anionic pollutants from wastewater.

In another study, sulfur-functionalized graphene sheets (GSs) were prepared by diazotization of sulfanilic acid and then used in the removal of aromatics and positively charged heavy metal ions from wastewater [74]. The saturated adsorption capacities of GS were $400\ mg\ g^{-1}$ for phenanthrene, $906\ mg\ g^{-1}$ for MB, and $58\ mg\ g^{-1}$ for Cd(II) ions, which were much higher than those obtained by rGO and GO owing to the presence of multiple adsorption sites such as π-e interactions and electrostatic interactions with functional groups created on GS.

To improve the recovery and adsorbing capacity of graphene, graphene aerogels were prepared and applied successfully in selective separation of emulsified oil from wastewater. This macrostructural form of graphene ensured the recovery of adsorbents for reuse applications [5]. To utilize the benefits of macrostructured graphene, 3D porous graphene hydrogels (GHs) with super adsorption capacity for different types of pollutants (antibiotics, dyes, and heavy ions) were prepared and used effectively in wastewater treatment [75]. The high porosity and water content both were considered responsible for the observed super adsorption capacity of GHs.

In these studies, it was also found that buried water in GHs played combinatorial roles such as in supporting media, transport in nanochannels, and hydrogen bonding, which promoted the adsorption of pollutants. This was due to strong interactions of GHs buried water with pollutants via hydrogen bonding than other types of water. The prepared GHs utilized the advantages of graphene including its high chemical resistance and excellent mechanical property and of hydrogel including its high water content, porous structure, simple solution-based processability, and scalability.

To enhance the adsorption properties of graphene, the zirconium hybrid of graphene was prepared and used as potential ion exchanger in theremoval of fluoride anions from wastewater [76]. To increase the selectivity of graphene in the elimination of Cr(VI) ions, recently the cyclodextrin-functionalized 3D graphene was developed, which provided an improved and selective separation of Cr(VI) ions from wastewater [77]. A graphene-based 3D hybrid composite adsorbent was also developed using MgO to enable an efficient adsorption of heavy metal ions from wastewater [78]. This 3D graphene architecture provided an opportunity for complete removal of graphene from treated water. The selectivity of graphene for mono- and divalent cations is also assessed by controlling the pore size in graphene [79].

To accomplish the need of an efficient adsorbent for the removal of organic dye pollutants, negatively charged and highly porous graphene/carbon nanotubes hybrid beads (HPGCBs) with strong mechanical stability were prepared. These beads proved to be an efficient adsorbent in removal of dyes as their activation was accomplished in the presence of KOH. The KOH activation created lots of nanopores (0.8–2 nm) on the graphene network, which created a large specific surface area ($1270\ m^2g^{-1}$) to exhibit a maximum adsorption capacity of $521.5\ mg\ mL^{-1}$ for MB [80]. Some studies indicated an exponential increase in the uptake of cationic pollutants on increasing the oxygen functionalities on graphene surfaces [81]. In a recent study, the graphene composites exhibited high photocatalytic activity on adding titania, hence might be suitable in degradation of dyes and organic pollutants of wastewater [82].

Resilient graphene aerogels (GAs) with high emulsified oil adsorption capacities, excellent rebounding performance, oil-water selectivity, and recycling abilities were prepared and used efficiently in the selective separation of oils from emulsified diesel oil due to their high oil selectivity [83]. These graphene aerogels have a maximum adsorption capacity of $2.5 \times 10^4\ mg\ g^{-1}$ for emulsified diesel oil through physical interactions and were used repeatedly for at least ten times without any loss in their adsorption capacity.

Three-dimensional graphene foams were prepared using the seashell-based chemical vapor deposition (CVD) technique [84], which shown 250-fold weight gain properties for various types of oils and organic solvents. These 3D graphene foams were also employed in the fabrication of binder-free, flexible Li-ion batteries, which have a capacity of $260\ mAh\ g^{-1}$. The construction of 3D graphene-based adsorbents was also tried in various studies as it is free from restacking of graphene nanosheets

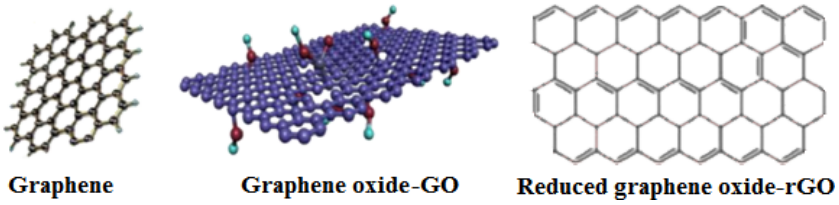

Figure 3. Graphene (G), graphene oxide (GO), and reduced graphene oxide (rGO).

but retains its intrinsic properties of 1D and 2D precursors during the adsorption process [85].

Biopolymers are the most commonly used adsorptive materials for water contaminants. Due to their advantageous adsorption properties, biopolymer-based graphene adsorbents were also developed with various biopolymers. Recently, chitosan spheres cross-linked graphene nanoplates (CS/GNPs) were prepared and applied in the efficient removal of methyl orange (MO) and AR1 anionic dye from wastewater [86]. The electrostatic interactions between dye molecules and amino groups of chitosan along with π-π interactions between the benzene ring of graphene and π-e electrons of dye molecules were considered responsible in the elimination of dye molecules from wastewater.

2.2.2 Graphene Oxide (GO)

The oxidation of graphene to GO contributes to its solubility in water due to the generation of oxygen-containing hydrophilic functional groups at its surfaces such as hydroxyl, epoxy, and carboxyl groups (Fig. 3). These oxygen-containing hydrophilic functional groups promote the adsorption of positively charged pollutants from wastewater [87]. Thus, GO was used in the removal of pollutants from wastewater.A few-layered GO (FGO) has been applied as an adsorbent in the elimination of Pb(II) ions with a maximum adsorptive capacity of 1850 mg g^{-1} of Pb(II) ions at 20 °C, which is much higher than of original graphene [88].

To evaluate the adsorption properties of GO in hybrid nanocomposites, GO-based hybrid nanocomposites with inverse spinel nickel ferrite (GONF) were prepared and used in the removal of Pb(II) and Cr(III) ions from wastewater by batch adsorption technique [89]. GONF nanocomposites showed a maximum adsorptive capacity of 25.0 mg g^{-1} for Pb(II) ions at pH 5.5 and 45.5 mg g^{-1} for Cr(III) ions at pH 4 and 25 °C. The maximum adsorptive capacity of GONF nanocomposites for Pb(II) and Cr(III) ions was determined by the Langmuir adsorption isotherm assuming monolayer chemisorption of metal ions on homogeneous surfaces of GONF nanocomposites. The maximum adsorptive capacity increased with higher adsorption temperature. This is an indicative of endothermic chemisorption by a process of complexation at inner-sphere surfaces of GONF nanocomposites. The GONF nanocomposites were recycled and reused at least for three cycles without any significant loss in their adsorptive capacities.

To remove the toxic Pb(II) ions from contaminated wastewater, GO-based self-propelled microboats (GOx-microboats) as adsorbent were prepared, which had nanolayers of GO and Pt/Ni layers to add a different functionality in microboats of GO [90]. The adsorbed Pb(II) ions were recovered from GO microboats by varying solution pH, and regenerated GO microboats were reused for decontamination of wastewater. The mobile GO microboats were able to remove 20 times more Pb(II) ions than stationary GO microboats by reducing the Pb(II) ions contamination down to 50 ppb in 60 min from the original 1000 ppb Pb(II) ions contamination.

In order to perform an effective separation of heavy metal ions such as Co(II), Ni(II), Cu(II), and Zn(II) ions from wastewater, pressed and unpressed GO/cellulose composite membranes were fabricated and used for separation of Cd(II) and Pb(II) ions [91]. The pressed membranes were found to be quite stable during separation of heavy metal ions as a function of solution pH and simultaneous vigorous stirring solution. Unpressed membranes exhibited low stability during adsorption. However, they were used successfully in filtration processes even at high flow rates. Results also indicated a maximum separation of metal ions within a pH range of 4–8. The affinity of these membranes in the separation of various metal ions had the following order: Pb > Cu > Cd > Zn ≥ Ni ≥ Co.

GO-chitosan-poly(vinyl alcohol) hydrogels were used successfully in the removal of Cd(II) and Ni(II) ions from aqueous solution. The recovery of adsorbed ions was accomplished by varying the swelling ratio of hydrogels [11]. The application of GO as hydrogel ensured a complete removal of adsorbent from water after treatment.

The zirconium- and phosphate-functionalized GO nanocomposites (GO-Zr-P) were prepared and employed in the elimination of Pb(II), Cd(II), Cu(II), and Zn(II) ions from wastewater [92]. In these nanocomposites, the flat and layered portion of GO was varied due to added zirconium and phosphate. On addition of zirconium and phosphate, the prepared sheets of GO-Zr-P nanocomposites became strongly wrinkled, which increased their adsorptive capacity for Pb(II), Cd(II), Cu(II), and Zn(II) ions in comparison to pristine GO. The metal ions removal efficiency of GO-Zr-P nanocomposites was about 99 % within a period of 20 min [92].

A combined approach of experimental and molecular dynamics simulation was selected by Sarupria and co-workers for the remediation of polycyclic aromatic hydrocarbon contaminants by third-sixth generation polyamidoamine (G3-G6-PAMAM) dendrimers and GO at its different oxidation states [93]. The cooperative interactions of naphthalene with dendrimers and GO enhanced the removal of naphthalene from wastewater. The intramolecular interactions in naphthalene molecules also influenced the adsorptive capacity of the adsorbent.

To prevent the aggregation of magnetic GO (mGO) and to increase its adsorptive capacity, EDTA-functionalized mGO (EDTA-mGO) was also prepared and found to be an efficient adsorbent in the removal of Pb(II), Hg(II), and Cu(II) ions from water in comparison to the EDTA complex of GO (EDTA-GO), ferric oxide (EDTA-Fe_3O_4), and mGO alone [94]. The chelating property of EDTA, increased electrostatic interactions with abundant oxide functionalities [95] on GO (Fig. 3), and magnetic properties of mGO in complex all together increased the adsorptive capacity of the EDTA-mGO complex in the elimination of Pb(II), Hg(II), and Cu(II) ions from wastewater. The EDTA-mGO complex was separated easily due to its magnetic properties. The maximum adsorptive capacity for Pb(II), Hg(II), and Cu(II) ions was found to be 508.4, 268.4, and 301.2 mg g^{-1}, respectively, as determined by the Langmuir isotherm. The adsorption of these metal ions was proposed to be endothermic in nature.The GO-based membranes were also applied for the separation of natural organic matters (NOMs), which are always left over in wastewater after water treatment [96]. In this study, a treated wastewater with ~ 5 mg L^{-1} dissolved organic carbon (DOC) was taken, which

was reduced to ≤ 5 ppb after permeation of wastewater through GO membranes at a flux rate of 65 $L\,m^{-2}h^{-1}bar^{-1}$ under atmospheric pressure. This suggested that GO membranes were able to remove > 99.9 % of dissolved NOMs from treated wastewater.

Like hybrids of graphene, the hybrids of GO monolayer decorated with magnetic manganese ferrite nanoparticles were also prepared and used in the removal of Pb(II), As(III), and As(V) ions from wastewater [97]. The GO hybrids exhibited a maximum adsorption capacity of 673 $mg\,g^{-1}$ for Pb(II) ions, 146 $mg\,g^{-1}$ for As(III) ions, and 207 $mg\,g^{-1}$ for As(V) ions from wastewater [97]. GO hybrid absorbents were also employed in simultaneous removal of multiple heavy metal ions from wastewater due to multifunctional properties of their surfaces.

Moodley and co-workers utilized four adsorbents, i.e., MCM-41, ASM41, and conjugates of GO (MCM-41-GO) and reduced GO with MCM-41 (MCM-41-rGO). The conjugated adsorbents were applied in the removal of acetaminophen and aspirin from wastewater [98]. The GO and rGO encapsulated in mesoporous silica (MCM-41) displayed improved adsorption capacity and also helped in separation after completion of adsorption. The effect of adding a surfactant template (CTAB) to ASM41 was also studied for the removal of acetaminophen and aspirin from wastewater. The influence of various parameters such as solution pH, initial concentration, contact time, and adsorbent dose on the adsorption of acetaminophen and aspirin in batch adsorption process was also examined. ASM41 and MCM-41-rGO had a maximum adsorptive capacity of 909.1 $mg\,g^{-1}$, and 555.6 $mg\,g^{-1}$ for aspirin and acetaminophen, respectively. These adsorbents were regenerated easily for their reuse applications.

Phosphorylated graphene oxide (PGO-400) was prepared by reacting GO with phosphorus trichloride and triethylamine in THF. It was found to be a renewable and recyclable adsorbent in the removal of Rhodamine-B (RhB) from wastewater [99]. The extraordinary characteristics such as electronic, thermal, cation-exchange, and water dispersibility properties together were considered responsible for the increased efficiency of the prepared PGO-400 adsorbent.

GO nanosheets were also used as a versatile de-emulsifier to destabilize the oil-in-water emulsion at ambient conditions [100]. The easy de-emulsification was an indicative for the presence of a low amount of residual oil in separated water ($< \sim 30$ $mg\,L^{-1}$). By using the optimum amount of GO, a de-emulsification efficiency of over 99.9 % can be achieved. The de-emulsification ability of GO was due to strong interactions between GO nanosheets and asphaltenes/resins molecules. The distribution of GO nanosheets in oil or water phase after de-emulsification proved to be dependent on the solution pH or on the resultant amphiphilicity of GO nanosheets, which also varied with solution pH.

The crumpled graphene oxide (CGO) is quite different in its aggregation properties than GO. A multifunctional porous nanocomposite of crumpled 3D graphene oxide was synthesized and used to fabricate advanced water treatment membranes by Fortner and co-workers [101]. The CGO is highly resistant to aggregation and compression (i.e., π–π stacking-resistant), hence it permits the entry of other multifunctional particles in its 3D structures. The monomeric CGO was mixed with TiO_2 (CGOTI) and Ag (CGOAg) to form composite nanoparticles, which displayed high separation efficiencies for model organic and biological foulants.

The multifunctionality of CGOTl was further demonstrated by studying in situ photocatalytic degradation of MO under fast flow conditions. CGOAg composites showed excellent antimicrobial properties for both biofilms and suspended growth microbes in wastewater. Polyaniline (PANI)-based composites of GO were also prepared and evaluated for their adsorption capacity for Pb(II) ions, exhibiting high adsorptive capacity for Pb(II) ions (1461 $mg\,g^{-1}$) in comparison to pristine GO (555 $mg\,g^{-1}$) or PANI (625 $mg\,g^{-1}$) at 25 °C [102]. The prepared nanocomposites removed dyes and heavy metal ions successfully from wastewater. The adsorption of heavy metal ions and dyes by GO-PANI composites followed the Langmuir model.

Clay composites of GO were also made by reinforcing GO and bentonite clay in hydrogels of polyvinyl alcohol (PVA)/carboxymethyl cellulose (CMC), which showed enhanced adsorption capacity for MB (172.14 $mg\,g^{-1}$) from wastewater in comparison to hydrogel (83.33 $mg\,g^{-1}$) at 30 °C [103]. This was ascribed to the high surface area of GO and interactions between MB and GO in the prepared composites. The adsorption of MB hydrogels followed pseudo-second-order kinetics, and the data fitted well to the Langmuir adsorption isotherm.

Like graphene, GO nanosheets were also applied to prepare composites with chitosan to take the benefit of naturally occurring biopolymer in adsorption of pollutants from wastewater. The electrostatic interactions between –OH groups of picric acid and amino groups of chitosan, and hydrogen bonding all together have increased the adsorption of picric acid on these nanocomposites. The application of chitosan influenced the surface area, total pore volume, and pore size of GO nanosheets that helped in adsorption of picric acid at nanocomposites [104]. These studies indicated that GO is more efficient in the removal of heavy metal ions in comparison to organic pollutants. This was due to the presence of a large amount of oxygen-containing groups at the surface of GO in comparison to graphene and rGO.

2.2.3 Reduced Graphene Oxide

Reduced graphene oxide (rGO) is another form of graphene and produced by chemical reduction of GO in the presence of various types of reducing agents such as sodium borohydrate, hydrazine hydrate, amino acids, pyrrole, ascorbic acid, and urea. The adsorption properties of rGO depend on defects/edges and oxygen-containing functional groups. Similarly to GO, the π–π interactions, hydrogen bonding, electrostatic interactions, or van der Waals forces of attractions influence the adsorption of pollutants on rGO. Like graphene and GO, the rGO also follows the Langmuir adsorption isotherm and pseudo-second-order kinetics. Many studies have confirmed that rGO is also an excellent adsorbent for the removal of heavy metal ions and organic pollutants. The π-π interactions between the graphene skeleton of rGO and aromatic moieties of malachite green (MG) dye and electrostatic interactions of residual oxygen functionality of rGO with π-e clouds with

positive centers of the MG dye influenced the adsorption of MG dye on rGO [87].

Studies indicated that noncovalent and charge interactions are stronger between rGO and the anionic dye (MO) in comparison to interactions with a cationic dye (MB) [105]. Similarly, the adsorption of pharmaceuticals from industrial effluents on rGO is predominated by hydrogen bonding between O/H of adsorbent and H/O and nitrogen/sulfur-containing groups (electron-rich elements) on pharmaceutical adsorbates [106], though π–π and electrostatic interactions contribute equally to the adsorption of pharmaceuticals.

To prevent the agglomeration of rGO to graphene during adsorption due to interplanar interactions and stacking, the rGO nanosheets were modified with CTAB (rGO/CTAB) and used successfully in the adsorption of anionic dyes (DR80 and DR23) from contaminated water as CTAB facilitated the interactions between dyes and rGO [107]. The recovery of rGO nanosheets from wastewater for reuse applications is a challenging task; hence, integration of magnetic nanoparticles (Fe_3O_4) was carried out to expedite the recycling of adsorbent. To overcome this problem, the nanocomposites of rGO using ferric oxide (rGO-Fe_3O_4) were prepared by the one-pot method, and provided a maximum adsorption capacity of 30.68 mg g^{-1} for Pb(II) ions from wastewater [108]. The nanocomposites after adsorption were recovered in a fast process. In a similar kind of studies, the Fe_3O_4-rGO nanocomposites were prepared and used as efficient adsorbents in the removal of various pesticides from wastewater.

The electrostatic [95] and π-π interactions [13] are principally considered responsible for the adsorption of pesticides and other contaminants on rGO-Fe_3O_4 nanocomposites. The possible interactions of rGO with pollutants were explained by taking MB dye molecules as an example (Fig. 4). The oxygen-containing groups on rGO influence the interactions between rGO and positively charged Pb(II) ions [87] similarly to GO (Fig. 3).

To enhance the adsorptive capacity of rGO and to facilitate its separation after adsorption, nanoparticles of rGO composites with cobalt oxide (rGO-Co_3O_4) were prepared by a one-step method under mild conditions [109], which showed a

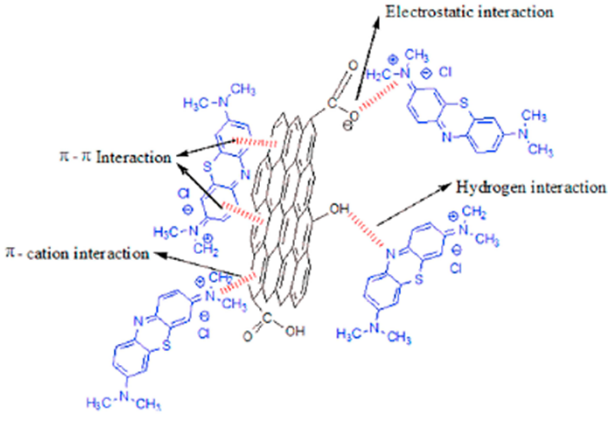

Figure 4. Possible interactions of rGO responsible for adsorption of pollutants as explained taking as methylene blue dye as typical example.

maximum adsorption capacity of 208.8 mg g^{-1} for Cr(VI) ions from wastewater. These composite nanoparticles were separated easily by using a magnet as they are ferromagnetic in nature. For the removal of Cr(VI) ions, Yu and co-workers also synthesized rGO nanocomposites with nickel oxide (rGO/NiO) at room temperature, which were highly adsorptive in the removal of Cr(VI) ions at pH 4.0 and 25 °C [110].

In another approach of surface functionalization of rGO, grafting of thymine on rGO was carried out, which increased the selectivity of rGO for the adsorption of Hg(II) ions as compared to pristine rGO [111]. This enhanced affinity of thymine-grafted rGO for Hg(II) ions is attributed to the formation of an rGO-thymine-Hg(II) complex, which increased the adsorption capacity of Hg(II) ions to 128 mg g^{-1} from 60 mg g^{-1} on pristine rGO. The adsorption of Hg(II) ions on the rGO-Thy complex followed pseudo-second-order kinetics and the rGO-Thy complex allowed for 100 % efficiency in the removal of Hg(II) ions from wastewater. The adsorption capacity of the rGO-Thy complex remained unchanged up to four cycles without an obvious decrease in its adsorption capacity for Hg(II) ions. The volume of actual industrial wastewater treated with the rGO-Thy complex in a fixed-bed column was found to be significantly high (390 BV) for the removal of Hg(II) ions, which indicated that rGO-Thy complex was quite efficient and scalable to design a water treatment plant that can be used for the handling of a civil sewage system.

The metal ion doping technique is also applied to increase the active sites on rGO as adsorbent. To evaluate the metal ion doping effect, Mn-doped TiO_2 was grown at the surface of rGO by the one-pot hydrothermal method and used successfully in photocatalytic removal of Cr(VI) ions in the presence of sunlight [112]. The deposition of Mn-doped TiO_2 on rGO surface displayed an increased removal efficiency of 97.32 % for Cr(VI) ions in 30 min and 99.02 % in 60 min in the presence of sunlight. The synergetic effect of rGO in adsorption of Cr(VI) ions and photocatalytic activity of Mn-doped TiO_2 in reducing Cr(VI) ions finally improved the efficiency of rGO for the removal of Cr(VI) ions from wastewater. The high photocatalytic activity of Mn-doped TiO_2 in reduction of Cr(VI) ions in the presence of sun light is mainly attributed to Mn doping. This process of Mn doping created abundant photocatalytic sites of Mn-TiO_2 on the rGO surface which improved its photocatalytic efficiency. In this study, the adsorbed Cr(VI) ions were first reduced to Cr(III) ions by photoelectrons that were transported through the rGO and the resultant Cr(III) ions remained adsorbed at the surface of rGO.

To evaluate the effect of porosity in the adsorption of the adsorbate on rGO, Wang et al. [113] fabricated superhydrophobic and superoleophilic porous reduced graphene oxide/polycarbonate (rGO/PC) monoliths having micro-nanoscale binary structures via thermally impacted nonsolvent-induced phase separation (TINIPS) method. The porous rGO/PC monoliths showed excellent capacity and selectivity in the absorption of a wide range of oils and organic solvents from wastewater. Furthermore, these monoliths also displayed a strong stability against acidic and alkaline media.

To prepare nanocomposites of rGO with core shell structures, recently, novel core@shell composites of rGO were prepared by an alternate assembly of titania nanosheets (TNS) and

rGO on coal fly ash (CFA) microspheres via the layer-by-layer self-assembling process [114]. The synthesized core@shell composites (CFA@(rGO/TNS)$_n$) were applied successfully in the photodegradation of MB by UV irradiation. The tight wrapping of TNS and rGO on the CFA surface reduced the recombination of electrons and holes charge carriers. The photocatalytic activity of nanocomposites depends on the number of wrapped layers of rGO/TNS core shell nanocomposites on CFA. The rGO in the nanocomposites helped in providing a large surface area, in causing fast transfer of charge carriers, and in reducing the rate of recombination of charge carriers, which ultimately improved the light harvesting efficiency of the prepared core-shell nanocomposites.

Like fly ash, the cellulose acetate membrane is also used as a support for rGO composite membranes. In this approach, polydopamine (PDA)-modified composite membranes of rGO/halloysite nanotubes (rGO/HNTs) were fabricated on commercial cellulose acetate (CA) membranes (PDA/rGO/HNT-CA) by Liu et al. [115]. The flux of wastewater from PDA/RGO/HNT membranes indicated a significant improvement on increasing the amount of HNT in composite membranes. In these composite membranes, the dopamine was used to strengthen the adhesion between rGO and HNT. The polydopamine-modified rGO/HNT membranes exhibited a high adsorption capacity for dyes, heavy metal ions, and were highly efficient in the separation of oils from emulsions. The retention of MB, congo red (CR), Cu(II), and Cr(III) ions by polydopamine-modified rGO/HNT membranes was 99.72 %, 99.09 %, 99.74 %, and 99.01 %, respectively, and the oil separation rate from emulsion was about 99.85 % on using 0.15 g PDA/RGO/HNT membranes. The high retention efficiency for MB and CR was attributed to the enhanced adsorption by rGO/HNT membranes due to the difference in electronegativity and physical sieving effects. The high retention efficiency for Cu(II) and Cr(III) ions was assigned to the presence of electrostatic attractions and to the possibility of ion exchange and surface complexation. These HNT-reinforced membranes of rGO also retained high antifouling properties even after three cycles.

Graphene (G), GO, and rGO nanosheets were also employed for adsorption of nitroaromatic explosives (NACs) including *m*-dinitrobenzene, nitrobenzene, and *p*-nitrotoluene [116]. The hydrophilic GO nanosheets showed the lowest adsorption capacity for explosives but rGO nanosheets displayed the highest adsorption capacity due to the presence of more defect sites than GO or G nanosheets, which was 10–50 times greater than CNTs. Various interaction modes including π-π electron donor-acceptor interactions between π-electron-deficient phenyls of NACs and the π-electron-rich matrix of graphene, and electrostatic and polar interactions between oxygen-containing groups/edges/defects of graphene and $-NO_2$ groups of NACs led to improved adsorption of NACs.

To analyze the effect of ionic strength of wastewater on adsorption of water pollutants, the adsorption of sodium dodecylbenzenesulfonate (SDBS) on rGO was studied [45]. The adsorption of SDBS on rGO was completed in much shorter time from aqueous media in the presence of sodium chloride, and adsorption was explained by proposing a dual site mechanism.

To evaluate the effect of biopolymers, the adsorption properties of biopolymer-modified rGO were investigated, which varied significantly with the properties of the solvents. This provided another way to influence the adsorption properties of adsorbents by taking different types of solvents. To analyze the effect of solvent properties on adsorption, the adsorption studies were carried out by varying the self-assembled structures of biopolymers in the presence of different solvents [117]. The adsorption properties of biopolymer-modified rGO exhibited variation due to differences in self-assembled structures of chlorophills on the surface of rGO.

These studies clearly indicate that rGO is a potential adsorbent and may be used effectively in the treatment of wastewater. Like other derivatives of graphene, the adsorption properties of rGO are largely influenced by various parameters such as defect sites, which are comparatively more in rGO than GO.

2.2.4 Graphitic Carbon Nitride

Graphitic carbon nitride (g-C_3N_4) is the most stable allotrope of polymeric carbon nitride stacked with 2D structures. It is thermally and chemically stable along with high biocompatibility and also used as medium-gap (2.7 ev) organic semiconductor. This environmentally benign material is prepared easily and only made of carbon and nitrogen elements. These properties have qualified g-C_3N_4 for diverse applications, such as for the removal of pollutants and to act as metal-free photocatalyst in the treatment of wastewater [118, 119]. The g-C_3N_4 derived from urea possesses a larger surface area (40 m^2g^{-1}) than that obtained from dicyandiamide and melamine (37 m^2g^{-1}). The g-C_3N_4 synthesized from urea (UCN) has a larger pore size than g-C_3N_4 synthesized by melamine (MCN). The g-C_3N_4 develops a negative charge at its surface in aqueous solution that facilitates the adsorption of cationic dyes (MB) and metal ions [120, 121]. It has a sheet-like morphology with a thickness of ~ 1–10 nm and lateral thickness of ~ 1–3 µm. The g-C_3N_4 nanosheets with high surface area (~ 109 m^2g^{-1}) and abundant surface active sites are conducive for photocatalytic decomposition of pollutants in wastewater [122].

The morphology of g-C_3N_4 varies on using different precursors for its synthesis [120]. In comparison to defect-free g-C_3N_4, the defect-rich g-C_3N_4, electron-rich nitrogen atoms and the presence of functional groups all together facilitate the adsorption of pollutants at its surface and enhance the photocatalytic activity of g-C_3N_4 in degradation of pollutants [123]. The better applicability of the Langmuir adsorption model in adsorption of organic dyes on g-C_3N_4 suggested the presence of a homogeneous monolayer of dye molecules at the surface of g-C_3N_4 [120]. However, in contrast to cationic dyes, the adsorption of heavy metal ions such as Pb(II) ions followed the Freundlich adsorption model better than the Langmuir adsorption model [121].

The increased adsorption of Pb(II) ions on g-C_3N_4 at high pH is ascribed to the increased negative charge density at its surface due to the formation of OH^- ions, which increased electrostatic interactions with metal ions in the treatment of wastewater. The adsorption of Pb(II) ions followed pseudo-second-order kinetics. The g-C_3N_4 is also used in the development of selective hydrogels for the treatment of water. The hydrogels exhibited improved selective adsorption of cationic dyes due to

increased negative charge and surface area ($190\ m^2g^{-1}$) of g-C_3N_4 in hydrogels in comparison to pristine g-C_3N_4 ($\sim 50\ m^2g^{-1}$) [124]. The observed adsorption selectivity of hydrogel for cationic dyes is found useful in the elimination of cationic dyes from a mixture of cationic and anionic dyes and also in the removal of gel after completion of the adsorption process.

In addition to 3D hydrogel structures, composites of g-C_3N_4 were prepared that allowed for increased photocatalytic decomposition of organic pollutants in comparison to pure g-C_3N_4 [125]. To enhance the interactions with the adsorbate, g-C_3N_4 is produced with improved oxygen functionalities, which showed better dispersion and efficient removal of pollutants from wastewater [126].

Besides adding surface functionality to g-C_3N_4, architectural modifications in g-C_3N_4 [127] such as porosities were also introduced to enhance its efficiency in the removal of pollutants by increased surface area and interactions with pollutants. These modifications were introduced by doping g-C_3N_4 with noble metals/metal ions, which led to improved photocatalytic decomposition of pollutants due to the larger surface area of g-C_3N_4 in comparison to pure g-C_3N_4 [128, 129]. The g-C_3N_4-based aerogels with enhanced porosity were also prepared using TiO_2 and graphene (g-C_3N_4-TiO_2-G), which provided an increased adsorptive and photocatalytic decomposition of RhB dye in aqueous solution in comparison to pure g-C_3N_4 [130]. This has been attributed to the higher porosity of g-C_3N_4 by added graphene (G) and due to the significant reduction in combinatorial charge carriers in TiO_2. Similarly to these studies, recently cellulose-derived hierarchical composites of g-C_3N_4 were also prepared in combination with TiO_2 (g-C_3N_4/TiO_2-nanotube), which displayed a higher photocatalytic activity than pure g-C_3N_4 [27].

To produce artificial enzymes or nanozymes based on g-C_3N_4, cobalt-doped graphitic carbon nitride (Co-g-C_3N_4) composites were fabricated by the one-pot thermal condensation method using urea and different amounts of cobalt chloride. With the addition of cobalt to g-C_3N_4, the prepared composites exhibited a higher peroxidase-like activity than pure g-C_3N_4. Based on the highly enhanced peroxidase-like activity, the Co-g-C_3N_4 composites were used to explore their applications in degradation of RhB in wastewater. The Co-g-C_3N_4 composites showed an eleven times higher rate of decomposition of RhB than in the presence of pure g-C_3N_4. These results led to the development of efficient artificial peroxidases for the removal of various types of contaminants from wastewater [131].

Recently, phenol-modified g-C_3N_4 was also created, which allowed for enhanced environmental remediation of different chromophoric organic pollutants in aqueous solution [15]. These studies clearly indicated that surface functionalization and hierarchical modification of g-C_3N_4 are the key factors that improve adsorptive and photocatalytic properties of g-C_3N_4 and can be used for the development of efficient adsorbents for the removal of pollutants from wastewater. Thus, g-C_3N_4 is a low-cost carbon nanomaterial with graphitic and high mechanical properties. The chemical and thermal stabilities of g-C_3N_4 also contribute towards its environmental friendliness in the removal of pollutants from wastewater. It has great potential to develop efficient adsorbents for the treatment of wastewater loaded with different types of organic and inorganic pollutants.

2.3 Activated Carbon and Nanoporous Carbon

2.3.1 Activated Carbon

The activated carbon (AC), also known as activated charcoal, is a low-cost material with high strength and easy regeneration properties. It is produced with characteristic micro/nanopores and large surface area ($> 3000\ m^2$) using various types of biomass such as rice husk, palm and coconut shells, tobacco stem, wood saw dust, pear seed cake, olive stones, bamboo etc. [132, 133] as well as from sewage sludge of civil municipalities after following some protocols [134].

Water treatment using AC is an efficient technique in comparison to traditional adsorbent-based techniques due to the ease of its availability, simplicity in its design and operation, and efficient capacity in removal of persistent dyes and pollutants from wastewater [135, 136]. AC is also employed in efficient removal of pesticides from treated drinking water. It is able to incorporate nanoscale features and due to its tailorable chemical properties it continues to remain one of the most favored adsorbent in water treatment techniques in many countries. AC plays a decisive role in removing contaminants such as organic constituents, residual disinfectants, fats, oils and grease, heavy metal ions from industrial wastewater [137], and for elimination of pharmaceuticals from wastewater of hospitals [138]. AC is also applied in water treatment plants to control the taste of water [139] and for removal of gases and odors [140]. In addition, AC is found useful in improving and protecting other water treatment processes, such as reverse osmosis and ion exchange separations, from possible damage to membranes due to oxidation or organic fouling.

The beneficial physicochemical and adsorbate-specific surface properties of AC (Fig. 5), such as specific surface area, pore size, and pore size distributions [141], have made AC an ideal adsorbent for the removal of pollutants from the effluents of different industries, e.g., pharmaceutics, fertilizer plants, petroleum, cosmetics, automobiles, and textiles [142]. The adsorption capacity of AC depends on its various textural properties such as surface area, porosity (Fig. 5), pore size, and charge on dye molecules.

The presence of functionalities and graphitic domains also influence the adsorptive properties of AC. Usually, AC is a

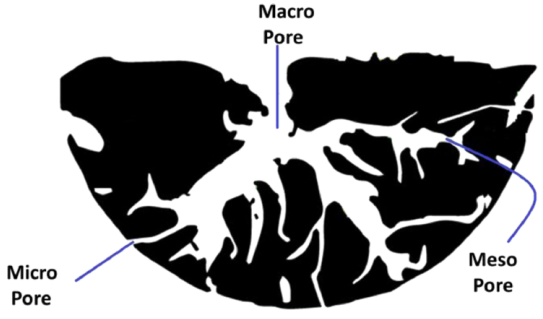

Figure 5. Types of pores in activated carbon.

highly porous material that helps in removal of contaminants from wastewater primarily through surface adsorption process [143]. Besides removing a variety of contaminants from wastewater, it is also capable for disinfection of water from bacteria and viruses [144]. Similarly, it is not only used in removing COD, BOD, and TSS of wastewater and as stabilizing agent but also in maintaining the optimum pH of water for the survival of aquatic life [145]. The adsorption capacity (%) of AC generally depends on contact time, pH, and temperature like other adsorbents. Its high mechanical strength makes it well-suited for periodic cleaning, regeneration, and reuse applications [133].

The AC produced through pyrolysis and chemical treatment of organic materials has pore diameters between > 50 to < 2 nm [146]. The adsorption at the surface of AC takes place via π–π interactions, hydrogen bonding, as well as with van der Waals forces [147]. The high surface-to-volume ratio in AC is also considered responsible for its improved ability to adsorb a large number of pollutants including various types of organic dyes and heavy metal ions [24]. As AC is reactivated easily, its low operational cost increases the return on investment (ROI) and ensures continuous operation of water treatment plants. Currently, AC is also used in point-of-use (POU) devices in commercial and home applications [148].

Though prepared graphene or AC-based composites for water purification are found costly and impractical for commercial sale, there is a high probability that composites may act as a platform to evolve the next-generation water purification method, with high performances and versatile capacities at POU.

AC proved also to be suitable in the treatment of wastewater streams with low concentrations of pollutants at extremely low cost and high efficiency due to the presence of large microporosity and surface area [149].

In some studies, two types of granular activated carbon (GAC) obtained from bituminous carbon (BC-GAC) and coconut shell (CS-GAC) were used in post-treatment processes of wastewater treatment plants (WWTPs) to enhance the elimination of left-over organic micropollutants (OMPs) [150]. The GAC filters were found versatile in selective removal of OMPs during the treatment of secondary effluents of different quality [150]. The AC, in combination with nanostructured metals, is also applied in the removal of organic pollutants from wastewater, with high adsorption efficiency and ease of separation from treated wastewater [151].

The AC obtained from civil sewage sludge is used efficiently in the elimination of Cu(II) ions from wastewater with a maximum adsorption capacity above 50 % [134]. The AC prepared from apricot stone is found suitable in the removal of Zn(II), Ni(II), Co(II), Cd(II), Cu(II), Pb(II), and Cr(III) ions from wastewater with a removal efficiency of above 97 % [152]. The AC carbon produced from pear seed cake was employed successfully for removing of MB with an adsorption capacity of 260 mg g^{-1} [153].

The chemical modification or formation of composites using AC proved to be effective methods in neutralization of harmful effects of water-borne pathogens [154].

Currently, a number of significant advancements have taken place to improve the water purification processes by modifying the treatment process based on ACs. In particular, the chemical modification of AC enhanced its adsorption efficiency for organic and inorganic pollutants [155]. The presence of oxygen and carboxylic functionality on AC promotes the adsorption of cationic dyes due to electrostatic interactions. Similarly, AC is produced with other functionalities through chemical modifications to improve its adsorptive properties. In this regard, the AC of civil sewage sludge was functionalized with sulfur and used successfully for the removal of Pb(II), Cd(II), Cu(II), and Ni(II) ions from wastewater. The adsorption capacity of sulfur-functionalized AC was found to be 238.1, 96.2, 87.7, and 52.4 mg g^{-1} for Pb(II), Cd(II), Cu(II), and Ni(II) ions, respectively [156]. The agricultural-based AC with multisized pores (MPAC) and large surface area provided adsorption capacities of 1.34, 1.07, 1.22, 0.97, and 0.93 mmol g^{-1} for Pb(II), Cd(II), Cu(II), Ni(II), and Zn(II) ions, respectively, from wastewater at 30 °C [157]. In another approach of AC application, composites of AC and zeolite were prepared and used to maintain the solution pH [145].

Advanced nanocomposites for efficient purification of wastewater were developed using CNTs, graphene, and AC [158]. These nanocomposites were also found useful in the fabrication of size-selective membrane filters for removal of pollutants by blocking their flow through the membranes [159].

Studies indicated that pristine and silver-impregnated ACs were efficient in removal of bromide and iodide ions from wastewater, i.e., removal of bromide ions by silver-impregnated AC (95 %) as compared to pristine AC (26 %) [160]. The AC impregnated with silver nanoparticles had an antibacterial effect in the treatment of wastewater [161, 162]. Iron-impregnated ACs had a high adsorptive capacity in the removal of various types of heavy metals ions, such as Ar(III), Ar(V), Hg(II), and Pb(II), in comparison to pristine ACs [163].

A green synthetic method to impregnate copper oxide in AC-based nanoparticles is developed using *Moringa oleifera* leaves extract. The copper oxide-impregnated AC nanoparticles were taken as an adsorbent in the removal of nitrate ions from wastewater with an adsorption capacity of 60 % at pH 2 and pH 5.5 [164]. As there are enough possibilities for leaching of impregnated metals from composites, metal-impregnated AC as adsorbent is not used in point-of-use water purification devices until metal leaching issue is not resolved.

A series of AC-based perovskite nanocomposites ($La_{1-x}Nd_xFeO_3$@AC) were developed for the treatment of wastewater through electrochemical decomposition of MO dye. The $La_{0.6}Nd_{0.4}FeO_3$@AC nanocomposite anode exhibited a removal efficiency of 99.81 % and 96.66 %, respectively, for MO and COD in 10 min [165].

The cobalt-doped ferrite nanocomposites of AC ($CoFe_2O_4$/NOAC) were synthesized by a facile autocombustion method, which showed a removal efficiency of > 80 % of dye at pH 6.5, within a time period of 55 min at room temperature with an adsorbent dosage of 50 mg [166]. The nanocomposites were separated easily due to their magnetic properties. Due to the high adsorption capacity and low cost of the prepared adsorbent, the nanocomposites were found to be well-suited and effective in the removal of AV49 from wastewater [166].

Carya peels-based AC was employed to prepare cobalt-doped ferrite nanocomposites ($CoFe_2O_4$/AC) by hydrothermal

method for efficient removal of Cr(IV) ions from wastewater [167]. A similar type of nanocomposites ($CoFe_2O_4$/AC) was generated by ultrasound method and applied successfully in the adsorptive removal of maxilon red [168]. These studies clearly indicated that species-specific surface affinity can be introduced on the surface of AC nanocomposites by selecting an appropriate method of their preparation.

An AC-based 3D nanocomposite fiber membrane as visible light photocatalyst was fabricated by a modified electrospinning process [169]. The electrospun mesoporous AC fiber membranes had a specific surface area of 184.8 m^2g^{-1} along with abundant mesopores. The prepared membranes were found to be highly adsorptive and photocatalytic in the removal of MO. These nanocomposite membranes were also applied for eliminating Cu(II) and As(V) ions from a simulated wastewater, having a removal efficiency of over 90 % for Cu(II) and As(V) ions. The prepared nanocomposite fiber membranes were reused for more than ten times without any variation in their properties; hence, they are suitable for the treatment of organic or heavy metal ions in wastewaters [169].

Photocatalytic composite nanoparticles based on AC and TiO_2 (TiO_2/AC) were employed in the degradation of RhB dye at room temperature in the presence of UV radiation [170]. The results indicated that anatase TiO_2 nanoparticles were distributed homogeneously at the surface of AC on calcination at 500 °C. The composite nanoparticles had an efficiency of 93.2 % in the removal of RhB. The morphological structures and photocatalytic activity of composite nanoparticles were dependent on the loading of TiO_2 [170]. The TiO_2 nanoparticles on AC in natural clay (NC) composites displayed a higher photocatalytic activity in the degradation of MG dye in aqueous medium on UV irradiation than TiO_2 alone [171]. However, the degradation of MG was found to be slightly more at high pH in the presence of TiO_2.

In some studies, the application of microwave heating was also tried as a viable method in the preparation of AC with significantly improved capacity for the removal of certain pollutants. The application of microwave heating is able to influence the surface area and pore size distribution in AC [172]. This method is quite beneficial in terms of low power consumption in the production of ACs in a short period.

These studies clearly indicated that AC is an efficient and cost-effective adsorbent in the removal of pollutants from wastewater in comparison to other adsorbents. AC was found to be efficient in the elimination of various adsorbates from wastewater and it can be prepared by using low-cost raw materials and by following simple protocols of its preparation. These attributes of AC have made it a preferred material for water treatment due to its wide availability, low cost, and low sensitivity to moisture. Its removal efficiency can be tailored by improving its surface area, pore size, pore structures, and pore size distribution. Similar to ACs, biochars also proved to be well-suited in wastewater treatment as indicated by magnetic biochar produced from discarded waste using microwave heating [173]. The prepared biochar had a maximum removal efficiency of 96.17 % for Cd(II) ions from wastewater, suggesting a suitable adsorbent comparable to AC.

2.3.2 Nanoporous Carbons

The nanoporous carbon (NPC) is like AC but without complete activation. The carbonaceous materials are mainly categorized as macroporous (pore size 50–1000 nm), mesoporous (pore size 2–50 nm), and microporous/nanoporous (pore size < 2 nm). If carbon is populated with nano-sized pores, then it is called nanoporous carbon. The carbonization of various precursors such as wood, coal, fruit peel, or polymers at high temperature or by chemical treatment methods allows to produce porous carbons with controlled surface area, porosity, and surface functionalities. The pore size also depends on the type of chemical agents used for activation. For example, $ZnCl_2$-impregnated carbon activation at 600 °C produces microporosity, whereas KOH-impregnated carbon activation under identical conditions yields carbon with high pore size distribution [174].

Generally, NPCs are synthesized via pyrolysis and physical and/or chemical activation at high temperatures [175]. However, the high-temperature activation is associated with some drawbacks such as creation of defects and graphitization, which are overcome by using hard or soft templates and by carrying out carbonization by thermosetting or thermally unstable compounds. The application of hard or soft templates also facilitates the synthesis of NPCs with controlled pore size distribution [176]. The hard template method usually needs presynthesized organic or inorganic templates, whereas the soft template method is based on creation of nanostructures via self-assembly of organic molecules. The amphiphilic surfactants and block copolymers are commonly employed in soft template-driven synthesis of NPCs.

The pore structures in carbon shown significant improvements on activation with microwave and steam as observed during the formation of magnetic Co-Fe-impregnated porous carbon obtained from rice straw [177]. This indicated that porous carbons of different pore sizes can be produced by microwave or steam activation for the removal of dyes or pollutants of different sizes usually present in industrial wastewater.

In a recent study, the Bengal gram beans husk (BGBH) was converted to graphene-like lamellar structures along with abundant micropores after chemical activation with KOH (BGBH-C-K) [178]. The resultant microporous carbon was found potentially useful in the removal of anionic dyes (i.e., MO) from wastewater. In these studies, the adsorption kinetics, equilibrium isotherm, and effect of temperature were studied to understand the adsorption of MO on BGBH. The BGBH adsorbent was also selected to investigate the adsorption of MG, MB, and Congo red (CR) dyes to examine the effect of pore size and surface charge of the studied dyes. The surface area and porosity of BGBH-C-K was compared with mesoporous carbons obtained in the presence of $ZnCl_2$ or $FeCl_3$ as activating agents (BGBH-C-Zn/Fe). The BGBH-C-Zn/Fe nanoporous carbon exhibited thick-sheet-like structures with wide pore size distribution.

2.4 Fullerene, Activated Carbon Spheres, and Carbon Quantum Dots

2.4.1 Fullerene

Fullerenes are the zero-dimensional spherical form of carbon nanomaterials made of a certain fixed number of carbon atoms arranged in pentagons and hexagons at their surfaces. They have a high surface area and are prepared easily by various cost-effective methods. They are environmentally friendly in their nature and possess electron-accepting properties, which make them attractive adsorbents for the removal of environmental pollutants from wastewater [179, 180]. The interactions of π-electrons of fullerene with contaminants have a driving force for the adsorption of pollutants from wastewater. Despite of potential properties of fullerenes as adsorbents, their applications in water treatment are reported scarcely.

The adsorption of pollutants on fullerenes is influenced by the size of its self-assembled structures. The nano-sized self-assembled aggregates of fullerene (C60) showed improved adsorption of 1,2-dichlorobenzene (1,2-DCB) and naphthalene in comparison to macro-sized fullerene aggregates [179]. It is believed that the adsorption of adsorbates on fullerene takes place due to penetrating properties of adsorbates in spaces/defects available on the surface of fullerene nanoclusters besides benefiting from the large surface area of fullerenes. The adsorption and desorption on fullerene exhibit the formation of a hysteresis loop, which is assumed due to the existence of two types of adsorptions of contaminants, one at the external surface and the other at internal surfaces of aggregates of the fullerene.

The trace amount of fullerenes in combination with other materials like AC, lignin, and zeolites was used to fabricate nanocomposites, which showed increased adsorptive properties for pollutants [181]. The addition of fullerene in composites increased the hydrophobic character, which made composites better adsorbents for pollutants and allowed for improved reuse application. Alekseeva et al. conducted a comparative study of fullerene and its nanocomposite with polystyrene for the removal of Cu(II) ions [182]. The adsorption of Cu(II) ions on fullerenes was explained by the Langmuir adsorption model. These studies indicated that fullerenes have the potential to develop as efficient adsorbents for the treatment of wastewater.

2.4.2 Activated Carbon Spheres

Activated carbon spheres (ACSs) belong to a zero-dimensional form of carbon nanomaterials, which display numerous advantages over powdered or granulated AC used as a support for the catalyst [183] or as an adsorbent [184]. The AC spheres have a large surface area ($2000\ m^2g^{-1}$), high micropore volume ($1.0\ cm^3g^{-1}$), minimum surface energy, controllable pore size distribution, high mechanical strength, smooth surfaces, and low moisture contents. The AC spheres are prepared in different sizes such as nano-, meso-, and microspheres for various applications. The common raw materials or precursors taken for the preparation of ACSs are pitch, polymeric resins, lignocellulose, and carbohydrates. The precursors are mostly carbonized at about 800–900 °C, and subsequent activation is carried either physically using steam/CO_2 or chemically with alkalis or acids.

The nitrogen-containing carbon spheres (NCSs) are prepared by activation of $ZnCl_2$-impregnated spheres of a polymer of *m*-phenylenediamine and hexamethylenetetramine. The as-obtained ACSs had a diameter of about 0.6–1.2 µm and high surface area ($1237\ m^2g^{-1}$) and were used successfully for the removal of Cr(VI) ions from wastewater [185]. The ACSs provided a maximum removal capacity of $279\ mg\ g^{-1}$ Cr(VI) ions at pH 2.0. The Cr(VI) ions removal efficiency of ACS reached to 99.9 % on using a dose of $12\ g\ L^{-1}$ in the treatment of real acidic electroplating wastewater. Further, ACSs exhibited a removal efficiency of > 90 % Cr(VI) ions at the end of repeated six runs.

Carboxyl-rich ACSs were prepared with a by-product of the pulp refining industry and used in eliminating Pb(II) and Cd(II) ions from wastewater [186], having adsorption capacities of 380.1 and $100.8\ mg\ g^{-1}$ for Pb(II) and Cd(II) ions, respectively. Magnetic and N/S co-doped ACS (N/S-MCMs/Fe_3O_4) were fabricated by the silica template method using cysteine and Fe_3O_4 as source of sulfur and magnetic properties [187]. The prepared ACSs had a maximum adsorption capacity of $74.5\ mg\ g^{-1}$ of Hg(II) ions from wastewater and ACSs were removed easily by an external magnetic field. The hydrothermally processed and chemically activated ACSs were applied for the adsorption of MB, MG, and RhB dyes [188] with maximum adsorption capacities of 3152, 1455, and $1409\ mg\ g^{-1}$ for MB, MG, and RhB, respectively. In addition, ACSs exhibited a good reusable property after five consecutive cycles.

ACSs with abundant oxygen-rich functional groups were synthesized by a simple hydrothermal method of carbonization of glucose precursor and were employed for adsorptive removal of Cd(II) ions and photocatalytic degradation of CR dye [189]. The prepared ACSs had a large surface area of $1125.91\ m^2g^{-1}$ and maximum adsorption capacities of 276.09 and $382.15\ mg\ g^{-1}$ for Cd(II) ions and CR, respectively. The photocatalytic degradation of CR was achieved with 95 % removal efficiency within 90 min. The adsorption data were fitted suitably to a Freundlich isotherm and adsorption kinetics were of pseudo-second order.

Recently, ACSs were also prepared by $ZnCl_2$ activation of a precursor prepared by the Mannich reaction between lignocellulose and polystyrene [190]. The prepared ACSs were applied successfully in the separation of Cr(VI) ions from wastewater, having a surface area and average pore size of $769.37\ m^2g^{-1}$ and 2.46 nm, respectively. The prepared ACSs had a maximum adsorption capacity of Cr(VI) ions of $227.7\ mg\ g^{-1}$ at an initial pH of 2 at 40 °C. At lower pH, the functional groups of the ACS surface were protonated by abundant hydrogen ions, which provided opportunities for electrostatic interactions with negatively charged $Cr_2O_7^{2-}$ ions. The adsorbed Cr(VI) ions were reduced to Cr(III) ions by electron donor groups of ACSs and remained adsorbed at the surface of ACSs. However, at high pH the ACSs became negatively charged; hence, the extent of Cr(VI) ion adsorption dropped to $19.42\ mg\ g^{-1}$ at pH 9.0. The adsorption kinetics and isotherm fitted well to Elovich and Langmuir models, respectively.

These studies clearly indicated that carbon nanomaterials in the form of spheres are efficient in adsorption and removal of pollutants from wastewater due to their large surface area and by added surface functionalities. This demonstrates that there is an abundant scope for further research to produce carbon spheres with controlled size and pore size distribution to act as selective adsorbent for the removal of pollutants from wastewater.

2.4.3 Carbon Quantum Dots

Carbon quantum dots (CQDs) are a class of carbon nanoparticles having a size of around 10 nm. They are less toxic, biocompatible, chemically stable, cost-effective, eco-friendly, with high water dispersibility, and are produced easily by a hydrothermal method using sustainable raw materials. The high surface area ($1690\ m^2g^{-1}$) and the presence of oxygen-containing functional groups at their surfaces makes them effective adsorbents for the removal of pollutants [191] and effective photocatalysts [192] for the degradation of pollutants in wastewater. CQDs associated with $ZnSn(OH)_6$ were used successfully as photocatalysts for the purification of water in the presence of visible sunlight [193].

The photocatalytic activity of CQDs in degradation of organic pollutants showed an increasing trend on supporting them at metal organic framework structures (NH_2-MIL-125) [194]. The photocatalytic activity of metal organic framework structures-supported CQDs (CQDs/NH_2-MIL-125) was evaluated by studying the decomposition of RhB solution ($10\ mg\ L^{-1}$) at 90 °C using UV irradiation, resulting in almost 100 % RhB removal within 120 min. CQDs also displayed increased photocatalytic activity when supported on $La_2Ti_2O_7$ [195]. These results revealed that the presence of CQDs reduced the recombination of electron-hole pairs, hence, the degradation capability of photocatalysts was increased significantly.

To overcome the challenge of fast recombination of charge carriers and limited light utilization, a binary composite was prepared by incorporating $BiVO_4$ on nitrogen-doped CQDs through π-π and hydrogen-bond interactions [196]. The prepared binary composite was employed as an efficient photocatalyst as electron transfer properties of CQDs increased the separation of charge carriers and reduced the rate of their recombination. The incorporation of $BiVO_4$ with nitrogen-doped CQDs improved the range of light utilization of photocatalysts from UV-light to visible-light region.

Similarly, CQDs were loaded on TiO_2 nanofibers (CQDs-TiO_2NFs), which allowed for 100 % degradation of MB dye in 95 min in comparison to 71 % degradation of MB in the presence of TiO_2 nanofibers in the same period [192]. The TiO_2 nanofibers were able to generate electron-hole pairs in visible light and CQDs played the role of acceptors and transporters for photo-generated electrons. This ultimately increased the photocatalytic activity of CQDs in decomposition of MB in wastewater.

To increase the efficacy of CQDs for the removal of organic and inorganic pollutants from wastewater, CQDs were also doped with nitrogen, which improved the interactivity between pollutants and CQDs by increasing the available surfaces and edges of CQDs for the adsorption of pollutants from wastewater [191]. The nitrogen-doped CQDs (N-CQDs) demonstrated an improved removal of Cd(II) and Pb(II) ions as 75 % and 37 %, respectively, from wastewater due to the combined effect of both nitrogen and oxygen functionality at the surface of N-CQDs.

In another study for the development of magnetic CQDs adsorbents, the nitrogen-doped CQDs (N-CQDs) were prepared using citric acid and dicyandiamide and conjugated with iron oxide (Fe_3O_4) [197]. The prepared conjugate of iron oxide and nitrogen-doped CQDs (N-CQDs-Fe_3O_4) were taken as adsorbent in the removal of Pb(II) ions from wastewater. The interaction of empty d-orbital of Pb(II) ions with lone pair of electrons on nitrogen of N-CQDs was considered responsible for the enhanced adsorption of Pb(II) ions on iron oxide conjugated N-CQDs from wastewater.

To improve the efficiency for the removal of pollutants and separation of CQDs after adsorption, polyethyleneimine-functionalized CQDs were used to fabricate a magnetic nanocomposite adsorbent using $MnFe_2O_4$ (PECQDs/$MnFe_2O_4$) [198]. The prepared nanocomposite provided a removal efficiency of 91 % for U(VI) ions despite of strong electrostatic repulsion between the positively charged surface of the nanocomposite and U(VI) ions in wastewater. This indicated that the residual oxygen-containing functionality of CQDs was able to overcome the electrostatic repulsion of U(VI) ions to show ultimate adsorption of U(VI) ions on the nanocomposite. The adsorption capacity of CQDs composites showed a decreasing trend on reducing the solution pH due to enhanced adsorption of protons in comparison to metal ions [199]. However, at higher solution pH, the adsorption was enhanced due to the formation of a negatively charged surface of the composites.

A composite with various functionalities was prepared using CQDs and zinc-aluminium layered double hydroxide ZnAl-LDH (CQDs/ZnAl-LDH) for the adsorption of Cd(II) ions [200]. The prepared composite had a maximum adsorption capacity of $12.60\ mg\ g^{-1}$ for Cd(II) ions in 20 min. The adsorption data fitted well with the Freundlich adsorption model indicating that the surface of composites was heterogeneous in nature. These studies suggested that CQDs are potentially useful adsorbents in the removal of heavy metal ions and are able to reach increased photocatalytic activity in the decomposition of organic pollutants from wastewater. The development of CQds composites with different functionalities and porosities may be a focus for further research for wastewater treatments.

3 Techniques of Removal of Pollutants

Although there are various processes for the removal of pollutants from wastewater, such as ion exchange, assimilation, complexation, reverse osmosis, biodegradation, flocculation, membrane filtration, chemical precipitation, biosorption, coagulation, predation/ingestion, and solvent extraction (Fig. 6), the process of adsorption is considered best due to its efficient removal of pollutants, cost effectiveness, and sensitivity in removal of trace levels of pollutants from wastewater [144, 201]. For adsorption of pollutants, the carbon nanomaterials showed great potential in the removal of organic and

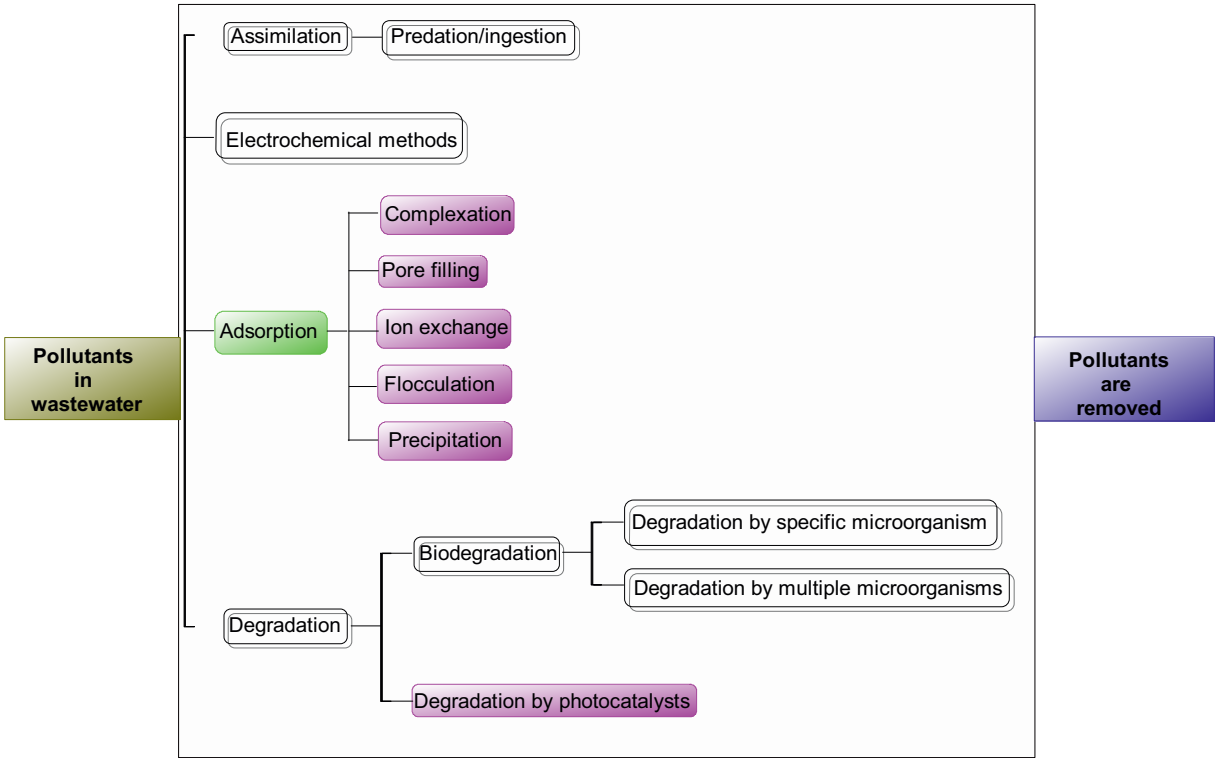

Figure 6. Pollutant removal processes.

inorganic pollutants from wastewater due to the presence of a large surface area, surface functionality, and recyclability of adsorbents. The chemical properties of carbon nanomaterials provide the control of various adsorption parameters such as loading capacity for pollutants, recovery of pollutant through variation of solution pH, and temperature. These properties of carbon materials make them efficient and preferred adsorbents in comparison to other adsorbents [202].

The degradation of pollutants using semiconductor-based carbon composites on irradiation with visible and ultraviolet radiations also opened a suitable way in the elimination of wastewater pollutants [203]. The spaces/defects in carbon nanoclusters and the low aggregation tendency of carbon-based nanomaterials make them appropriate and potential adsorbents in the removal of pollutants from wastewater [204].

3.1 Characterization of the Removal of Pollutants on Carbon Nanomaterials

The removal of organic and inorganic pollutants by carbonaceous materials is confirmed by evaluating the properties of adsorbents after adsorption by using one of the various techniques of characterization, such as X-ray diffraction (XRD), Fourier transformed infrared spectroscopy (FT-IR), UV-visible spectroscopy (UVS), X-ray photoelectron spectroscopy (XPS), electron microscopy (FESEM, TEM), atomic absorption spectroscopy (AAS), vibrating sample magnetic properties (VSM), gel permeation chromatography (GPC), differential scanning calorimetry (DSC), thermal analysis (TA), and by measurement of electrical conductivity of adsorbents after adsorption. These methods are able to provide in-depth information on structural variation or alternation in physical properties of the adsorbents after adsorption.

The evaluation of the residual amount of adsorbates in solution after adsorption is also employed to confirm the extent of adsorption that took place through interactions between adsorbents and adsorbates. These techniques are quite sensitive in exacting the amount of pollutants that has been adsorbed on the surface of carbonaceous materials.

To get information on the type of adsorption, the adsorption data are fitted in various adsorption models. The adsorption data of carbonaceous materials are frequently fitted in commonly used adsorption models such as Freundlich, Langmuir, and Dubinin-Radushkevich adsorption models to calculate the maximum amount of pollutants adsorbed per unit weight of carbonaceous adsorbent. The fitting of adsorption data in these models also is helpful to confirm the type of adsorption at the surface of absorbents or about adsorption that occurred through a pore adsorption process. Adsorption data help in ascertaining the types of interactions that were operating between adsorbents and pollutants. Besides the extent of adsorption, these data also are valuable in evaluating the type of kinetics that was followed by pollutants in the adsorption process. The adsorption data of pollutants on carbonaceous adsorbents mostly followed pseudo-first-order (PFO) and pseudo-second-order (PSO) kinetics as given by Elovich and demonstrated dependence on intraparticles diffusion (IPD) kinetic.

3.2 Mechanisms of Adsorption of Pollutants

The adsorption of pollutants on carbon materials takes place through various interactions as illustrated schematically in Fig. 7.

The physical adsorption of pollutants depends on the physicochemical properties of carbon adsorbents such as specific surface area, surface functionality, hydrophobicity, and due to various types of interactions, e.g., electrostatic, π-π, π-e, and hydrogen bonding. The adsorption of metal ions on carbonaceous materials usually takes place through various adsorption mechanisms like electrostatic interaction, ion exchange, complex formation [205], pore filling, hydrogen bonding, and π-hydrogen interactions [206]. The adsorption of organic pollutants occurs through hydrophobic interactions such as n-π and π-π electron donor-acceptor interactions, and Lewis acid-base interactions [69]. The π-π electron donor-acceptor interactions are observed during the adsorption process between target pollutants and aromatic regions of carbon nanomaterials (e.g., π-electron-depleted and π-electron-rich rings) [207, 208].

The adsorption of pollutants through pore-filling mechanism depends on the total pore volume of the porous network of the carbon nanomaterial and also is dependent on the size of pollutants [209]. The π-π stacking interactions are attributed to the sorption of aromatic compounds on the surface of carbon nanomaterials containing aromatic rings such as graphenes [210]. The electrostatic interactions are usually encountered during the adsorption of ionic and ionizable compounds on carbon nanomaterials [211]. The weak van der Waals forces of attractions and hydrogen bondings between functional groups on the carbon nanomaterial and functional groups of adsorbates are also considered responsible for the adsorption od pollutants on carbon materials. The ion exchange and complexation processes take place in the presence of organic cations or metal ions associated with the structure of carbon nanomaterials [212]. The ion exchange mechanism is the main mode of interaction between multivalent cations and carbon nanomaterials [213, 214].

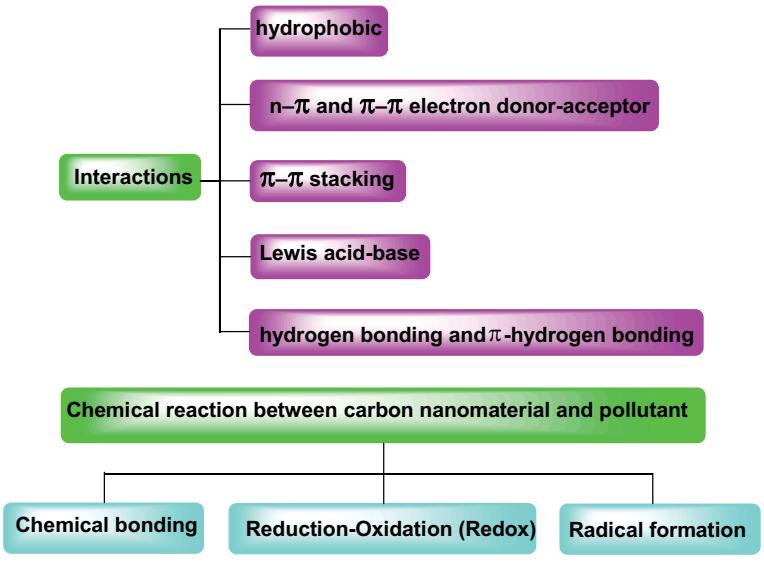

Figure 7. Mechanisms of removal of pollutants on carbonaceous materials.

The adsorption capacity of carbon nanomaterials depends on various parameters including surface functionalities, purity, porosity, surface area, density of active sites, type of carbon nanomaterials, and nature of pollutants. The adsorption of pollutants on carbon nanomaterials mainly occurs through chemical and physical interactions between adsorbents and pollutants at active sites including internal adsorption sites, interstitial channels, grooves, and active sites present on the external surface of carbon materials.

The mechanisms of adsorption of pollutants on carbon materials are discussed in various reviews available in literature. The adsorption mechanisms for the removal of inorganic pollutants from wastewater using graphenes and their derivatives are discussed in detail by Yusuf et al. [215]. It was indicated that surface area and pore size distribution in graphene, including total internal surface area, are important variables that influence the adsorption capacity of graphenes. The adsorption of pollutants on graphene also takes place due to π-stacking interactions besides hydrogen bonding [216]. The adsorption of anionic pollutants has been explained through electrostatic interactions and specific and nonspecific interactions that are prevalent at low pH [215].

The results of a comparative study for the removal of MB on various carbon nanomaterials, including AC, GO, and CNTs, indicated that the adsorption of MB on carbon-based adsorbents was influenced significantly by a large surface area, π-π electron donor-acceptor interactions, and electrostatic attractions between cationic dye and negatively charged adsorbents [217]. It was also stated that the adsorption might be a rate-limiting step for the exchange of electrons between adsorbent and adsorbate molecules. Solid-liquid separation mechanisms, such as flocculation and/or precipitation, are important processes, which are used by carbon nanomaterials in the removal of heavy metal ions from wastewater [218].

Various studies clearly revealed the effectiveness of carbon nanomaterials in the elimination of pollutants from wastewater. The removal of pollutants may also possible through adsorption and degradation processes at the surface of carbon nanomaterials. In some studies, the main mechanism of removal of pollutants is photocatalytic degradation as observed in the presence of g-C_3N_4 or CQDs, whereas the adsorption mechanism is considered as accessorial process [157, 209, 220].

The photocatalytic decomposition of organic pollutants takes place through a mechanism which is based on photoexcited electrons of the photocatalysts such as g-C_3N_4 or fullurene/CQDs and their composites which are able to generate holes (h^+) and exited electrons (e^-) in the conduction band. In aqueous media, the hydroxyl radicals are formed by the interaction of holes (h^+) with water molecules, which take part in oxidation of organic pollutants in wastewater [221]. Thus, carbon-based materials are able to remove pollutants by either one of the mechanisms or through a combination of two mechanisms depending on the properties of adsorbent and adsorbates.

4 Conclusions

The growing water pollution is a subject of great concern as it is causing scarcity of fresh and drinking water across the globe. Industrial effluents and domestic discharges are the prime sources of organic and inorganic pollutants such as dyes, pesticides, toxic heavy metal ions, fertilizers, and pharmaceuticals, which pose potential health hazards to human lives. Though various techniques have been used for the removal of pollutants and water-soluble dyes from wastewater, adsorption has been found to be an economically viable approach specially using carbon nanomaterials. These studies indicated that nanoforms of carbon such as graphene (G) and its derivatives (rGO) have outstanding properties in the removal of pollutants due to their favorable dimensional structures in comparison to low-dimensional nanocarbons such as CNTs, CNFs, CQDs, fullerene and ACS, which have limitations in terms of aggregation or restacking in solution during their applicatio.

To overcome these limitations of the low-dimensional form of carbon nanomaterials, the development of 3D nanostructures, such as composites and hydrogels of carbon nanomaterials, are the subject of current studies. However, this approach needs to be developed at large scale to overcone the existing challenges of aggregations and to retain their intrinsic properties such as porosity and large surface area for adsorption besides facilitating their separation from wastewater for reuse applications.

To enhance species-specific removal of pollutants from mixtures of multiple pollutant systems, surface functionalization needs to be encouraged, which is not yet practiced at large scale. Carbon nanomaterials with multiple surface functionalities may facilitate simultaneous removal of different adsorbates and their recoveries by controlling the pH or temperature-dependent interactions between adsorbates and functionalized carbon nanomaterials. Metal doping and activation processes need to be precised to control the surface area and hierarchical structures in carbon nanomaterials in order to improve the adsorptive properties and size selectivity for pollutants. Currently, activation of carbon nanomaterials is carried out at high temperature (< 500 °C); hence, activation methods need to be developed to affect the activation at low temperature in order to avoid the adverse effect of high-temperature activation on physicochemical properties of carbon nanomaterials.

In sum, the treatment of wastewater using different nanoforms of carbons provides ample opportunities for further research to improve their cost-effective efficiency in removal of pollutants in comparison to routinely used adsorbents.

Conflicts of Interest

The authors have declared no conflict of interest.

Hanna Abbo is a senior researcher in the Department of Chemistry, University of the Western Cape. She received her Ph.D. in Chemistry from Gurgula Kangri University in 2004. She is a Professor of the Department of Chemistry at Basrah University. Her research activities focus on the development of nanocatalysts for fuel cell, water treatment, and carbon utilization.

K. C. Gupta received his Ph.D. degree on Polymer Chemistry at the University of Allahabad in 1985 and is currently working as Professor at the Indian Institute of Technology Roorkee India. He is a recipient of several post-doctoral fellowships, Brain Pool award of South Korea, and Khosla National Research Award India. His research interests include functional polymers for sensing, catalysis, separation, and biomedical applications.

Nader G. Khaligh received his Ph.D. degree from the University of Guilan, Iran, in 2013. After two years at the Professor Reza Institute he moved to the Nanotechnology and Catalysis Research Study (University of Malaya) as a researcher. Since 2015 he is Senior Researcher of the University of Malaya. His research is focused on the heterogeneous and homogeneous catalysis, sustainable chemistry and energy, ionic liquids, and multi-task reagents.

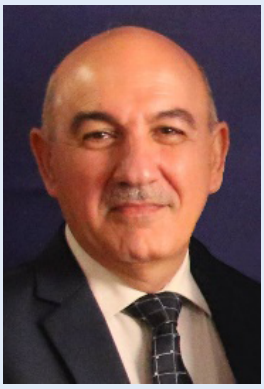

Salam Titinchi is a Professor of Inorganic Chemistry and Catalysis at the University of Western Cape. He obtained his Ph.D. from the Indian Institute of Technology, Roorkee, in 2004. His research interests are focused on the fields of heterogeneous catalysis, coordination polymers, and new anticancer compounds. Over the past years, new research directions have been established with a specific emphasis on advanced nanomaterials for energy and environmental applications, carbon capture and utilization, and surface-modified nanomagnetic materials for water treatment.

Abbreviations

AC	activated carbon
ACS	activated carbon sphere
BGBH	Bengal gram beans husk
CBZ	carbamazepine
CGO	crumpled graphene oxide
CGOTI	CGO mixed with TiO_2
CNF	carbon nanofiber
CNT	carbon nanotube
CR	Congo red
CS/GNP	chitosan spheres cross-linked graphene nanoplate
CTAB	cetyltrimethylammonium bromide
CVD	chemical vapor deposition
DOC	dissolved organic carbon
EDA	electron-donor-acceptor
FGO	few-layered GO
G	graphenes
GAC	granular activated carbon
GH	graphene hydrogel
GO	graphene oxide
GONF	GO-nickel ferrite
GS	sulfur functionalized graphene
HNT	halloysite nanotube
HPGCB	highly porous graphene/carbon nanotubes hybrid beads
MB	methylene blue
MC	methylthionine chloride
MG	malachite green
mGO	magnetic GO
MO-CVD	metal-organic chemical vapor deposition
MWCNT	multiwalled CNT
NAC	nitroaromatic explosive
NC	natural clay
NCS	nitrogen-containing carbon sphere
NOM	natural organic matter
NPC	nanoporous carbon
OMP	organic micropollutant
PAMAM	polyamidoamine dendrimer
PANI	polyaniline
PDA	polydopamine
PVA	polyvinyl alcohol
rGO	reduced graphene oxide
RhB	rhodamine-B
SDS	sodium dodecyl sulfate (anionic surfactant)
SWCNT	single-walled CNT
TEOS	tetraethyl orthosilicate
Thy	thymine
TNS	titania nanosheets

References

[1] S. Anisfeld, *Water Resources*, Island Press, Washington, DC **2011**.

[2] *Water Treatment Technologies for the Removal of High-Toxity Pollutants* (Eds: M. Václavíková, K. Vitale, G. P. Gallios, L. Ivanicová), Springer, Berlin **2008**.

[3] R. Noyes, *Unit Operations in Environmental Engineering*, Knovel, Norwich, NY **2006**.

[4] X. Huang, J. Tian, Y. Li, X. Yin, W. Wu, *Langmuir* **2020**, *36*, 10895–10904. DOI: https://doi.org/10.1021/acs.langmuir.0c00654

[5] C. Dai et al., *Langmuir* **2020**, *36*, 13698–13707. DOI: https://doi.org/10.1021/acs.langmuir.0c02664

[6] Z. Huang, Y. Zhao, B. Liu, S. Guan, J. Liu, *Langmuir* **2020**, *36*, 13708–13715. DOI: https://doi.org/10.1021/acs.langmuir.0c02761

[7] P. Atkins, *Elements of Physical Chemistry*, Oxford University Press, Oxford **2013**.

[8] A. Ahmad, M. Razali, M. Mamat, F. Mehamod, K. Anuar Mat Amin, *Chemosphere* **2017**, *168*, 474–482. DOI: https://doi.org/10.1016/j.chemosphere.2016.11.028

[9] A. Maleki et al., *Chem. Eng. J.* **2017**, *313*, 826–835. DOI: https://doi.org/10.1016/j.cej.2016.10.058

[10] J. Dwyer et al., *Langmuir* **2019**, *35*, 12492–12500. DOI: https://doi.org/10.1021/acs.langmuir.9b02217

[11] C. Li et al., *Langmuir* **2019**, *35*, 4481–4490. DOI: https://doi.org/10.1021/acs.langmuir.8b04189

[12] V. Uwamariya, Adsorptive Removal of Heavy Metals from Groundwater by Iron Oxide Based Adsorbents, CRC Press/Balkema, Leiden **2013**.

[13] M. Sadeghi, M. Tofighy, T. Mohammadi, *Chemosphere* **2020**, *253*, 126647. DOI: https://doi.org/10.1016/j.chemosphere.2020.126647

[14] M. Mauter, I. Zucker, F. Perreault, J. Werber, J. Kim, M. Elimelech, *Nat. Sustainability* **2018**, *1*, 166–175. DOI: https://doi.org/10.1038/s41893-018-0046-8

[15] M. Warshagha, M. Muneer, *Langmuir* **2020**, *36*, 9719–9727. DOI: https://doi.org/10.1021/acs.langmuir.0c01055

[16] J. Wang, Q. Zhou, Y. Shen, X. Chen, S. Liu, Y. Zhang, *Langmuir* **2019**, *35*, 12366–12373. DOI: https://doi.org/10.1021/acs.langmuir.9b01796

[17] S. Behera, C. Kim, K. Kim, *Langmuir* **2020**, *36*, 12494–12503. DOI: https://doi.org/10.1021/acs.langmuir.0c01906

[18] S. Abdulla, B. Pullithadathil, *Langmuir* **2020**, *36*, 11618–11628. DOI: https://doi.org/10.1021/acs.langmuir.0c02200

[19] H. Sadegh, R. S. Ghoshekandi, A. Masjedi, Z. Mahmoodi, M. Kazemi, *Int. J. Nano Dimens.* **2016**, *7*, 109–120. DOI: https://doi.org/10.7508/ijnd.2016.02.002
[20] Ihsanullah et al., *Sep. Purif. Technol.* **2016**, *157*, 141–161. DOI: https://doi.org/10.1016/j.seppur.2015.11.039
[21] A. Stafiej, K. Pyrzynska, *Sep. Purif. Technol.* **2007**, *58*, 49–52. DOI: https://doi.org/10.1016/j.seppur.2007.07.008
[22] M. Tofighy, T. Mohammadi, *J. Hazard. Mater.* **2011**, *185*, 140–147. DOI: https://doi.org/10.1016/j.jhazmat.2010.09.008
[23] Y. Yan, M. Zhang, K. Gong, L. Su, Z. Guo, L. Mao, *Chem. Mater.* **2005**, *17*, 3457–3463. DOI: https://doi.org/10.1021/cm0504182
[24] L. Prola et al., *J. Environ. Manage.* **2013**, *130*, 166–175. DOI: https://doi.org/10.1016/j.jenvman.2013.09.003
[25] C. Liu, J. Li, H. Zhang, B. Li, Y. Guo, *Colloids Surf., A.* **2008**, *313–314*, 9–12. DOI: https://doi.org/10.1016/j.colsurfa.2007.04.062
[26] R. Long, R. Yang, *J. Am. Chem. Soc.* **2001**, *123*, 2058–2059. DOI: https://doi.org/10.1021/ja003830l
[27] Z. Lin, B. Yu, J. Huang, *Langmuir* **2020**, *36*, 5967–5978. DOI: https://doi.org/10.1021/acs.langmuir.0c00847
[28] J. Yang, X. Jiang, F. Jiao, J. Yu, *Appl. Surf. Sci.* **2018**, *436*, 198–206. DOI: https://doi.org/10.1016/j.apsusc.2017.12.029
[29] M. Jahangiri, F. Kiani, H. Tahermansouri, A. Rajabalinezhad, *J. Mol. Liq.* **2015**, *212*, 219–226. DOI: https://doi.org/10.1016/j.molliq.2015.09.010
[30] S. Saber-Samandari, S. Saber-Samandari, H. Joneidi-Yekta, M. Mohseni, *Chem. Eng. J.* **2017**, *308*, 1133–1144. DOI: https://doi.org/10.1016/j.cej.2016.10.017
[31] H. Moghaddam, M. Pakizeh, *J. Ind. Eng. Chem.* **2015**, *21*, 221–229. DOI: https://doi.org/10.1016/j.jiec.2014.02.028
[32] D. Wan, L. Wu, Y. Liu, J. Chen, H. Zhao, S. Xiao, *Langmuir* **2019**, *35*, 3925–3936. DOI: https://doi.org/10.1021/acs.langmuir.8b04179
[33] M. Razali et al., *Green Chem.* **2015**, *17*, 5196–5205. DOI: https://doi.org/10.1039/c5gc01937k
[34] N. Hintsho, L. Petrik, A. Nechaev, S. Titinchi, P. Ndungu, *Appl. Catal., B* **2014**, *156–157*, 273–283. DOI: https://doi.org/10.1016/j.apcatb.2014.03.021
[35] B. Hayati, A. Maleki, F. Najafi, H. Daraei, F. Gharibi, G. McKay, *J. Hazard. Mater.* **2017**, *336*, 146–157. DOI: https://doi.org/10.1016/j.jhazmat.2017.02.059
[36] Z. Li, J. Chen, Y. Ge, *Chem. Eng. J.* **2017**, *308*, 809–817. DOI: https://doi.org/10.1016/j.cej.2016.09.126.Z
[37] M. Sweetman et al., *C* **2017**, *3*, 18. DOI: https://doi.org/10.3390/c3020018
[38] L. Yanyan, T. Kurniawan, A. Albadarin, G. Walker, *J. Mol. Liq.* **2018**, *251*, 369–377. DOI: https://doi.org/10.1016/j.molliq.2017.12.051
[39] R. Li et al., *Microchim. Acta* **2010**, *172*, 269–276. DOI: https://doi.org/10.1007/s00604-010-0488-9
[40] Y. Liu, Y. Li, X. Yan, *Adv. Funct. Mater.* **2008**, *18*, 1536–1543. DOI: https://doi.org/10.1002/adfm.200701433
[41] C. Jung et al., *Sep. Purif. Technol.* **2013**, *106*, 63–71. DOI: https://doi.org/10.1016/j.seppur.2012.12.028
[42] Y. Huang, X. Lee, M. Grattieri, F. Macazo, R. Cai, S. Minteer, *J. Mater. Sci.* **2018**, *53*, 12641–12649. DOI: https://doi.org/10.1007/s10853-018-2494-y
[43] R. Khakpour, H. Tahermansouri, *Int. J. Biol. Macromol.* **2018**, *109*, 598–610. DOI: https://doi.org/10.1016/j.ijbiomac.2017.12.105
[44] Y. Huang, X. Lee, F. Macazo, M. Grattieri, R. Cai, S. Minteer, *Chem. Eng. J.* **2018**, *339*, 259–267. DOI: https://doi.org/10.1016/j.cej.2018.01.133
[45] W. Anku, S. Oppong, S. Shukla, E. Agorku, P. Govender, *Appl. Phys. A* **2016**, *122*, 579. DOI: https://doi.org/10.1007/s00339-016-0086-8
[46] N. Mubarak, J. Sahu, E. Abdullah, N. Jayakumar, P. Ganesan, *J. Ind. Eng. Chem.* **2015**, *24*, 24–33. DOI: https://doi.org/10.1016/j.jiec.2014.09.005
[47] L. Jun, R. Karri, N. Mubarak, L. Yon, C. Bing, M. Khalid, P. Jagadish, E. Abdullah, *Environ. Pollut.* **2020**, *259*, 113940. DOI: https://doi.org/10.1016/j.envpol.2020.113940
[48] L. Jun, R. Karri, L. Yon, N. Mubarak, C. Bing, K. Mohammad, M. Khalid, P. Jagadish, E. Abdullah, *Environ. Res.* **2020**, *183*, 109158. DOI: https://doi.org/10.1016/j.envres.2020.109158
[49] L. Feng, N. Xie, J. Zhong, *Materials* **2014**, *7*, 3919–3945. DOI: https://doi.org/10.3390/ma7053919
[50] K. De Jong, J. Geus, *Catal. Rev.* **2000**, *42*, 481–510. DOI: https://doi.org/10.1081/cr-100101954
[51] B. Huang, J. Yue, Y. Wei, X. Huang, X. Tang, Z. Du, *Appl. Surf. Sci.* **2019**, *483*, 98–105. DOI: https://doi.org/10.1016/j.apsusc.2019.03.301
[52] Z. Liu, C. Zhao, P. Wang, H. Zheng, Y. Sun, D. Dionysiou, *Chem. Eng. J.* **2018**, *343*, 28–36. DOI: https://doi.org/10.1016/j.cej.2018.02.114
[53] M. Teng, J. Qiao, F. Li, P. Bera, *Carbon* **2012**, *50*, 2877–2886. DOI: https://doi.org/10.1016/j.carbon.2012.02.056
[54] Y. Ahmed, A. Al-Mamun, M. Al Khatib, A. Jameel, M. Al-Saadi, *Environ. Chem. Lett.* **2015**, *13*, 341–346. DOI: https://doi.org/10.1007/s10311-015-0509-3
[55] Y. Si, T. Ren, Y. Li, B. Ding, J. Yu, *Carbon* **2012**, *50*, 5176–5185. DOI: https://doi.org/10.1016/j.carbon.2012.06.059
[56] T. Ren et al., *J. Mater. Chem.* **2012**, *22*, 15919–15927. DOI: https://doi.org/10.1039/c2jm33214k
[57] Y. Si, T. Ren, B. Ding, J. Yu, G. Sun, *J. Mater. Chem.* **2012**, *22*, 4619–4622. DOI: https://doi.org/10.1039/c2jm00036a
[58] A. Gupta, D. Deva, A. Sharma, N. Verma, *Ind. Eng. Chem. Res.* **2010**, *49*, 7074–7084. DOI: https://doi.org/10.1021/ie100392q
[59] Z. Zhu et al., *Environ. Sci. Nano* **2017**, *4*, 302–306. DOI: https://doi.org/10.1039/c6en00568c
[60] K. Okada, N. Yamamoto, Y. Kameshima, A. Yasumori, *J. Colloid Interface Sci.* **2003**, *262*, 179–193. DOI: https://doi.org/10.1016/s0021-9797(03)00107-3
[61] X. Li et al., *J. Colloid Interface Sci.* **2015**, *447*, 120–127. DOI: https://doi.org/10.1016/j.jcis.2015.01.042
[62] D. Jha, N. Mubarak, M. Haider, R. Kumar, M. Balathanigaimani, J. Sahu, *Fuel* **2019**, *244*, 132–139. DOI: https://doi.org/10.1016/j.fuel.2019.01.006
[63] Y. Jiang, P. Biswas, J. Fortner, *Environ. Sci. Water Res Technol.* **2016**, *2*, 915–922. DOI: https://doi.org/10.1039/c6ew00187d
[64] M. Gandhi, S. Vasudevan, A. Shibayama, M. Yamada, *Chem. Select.* **2016**, *1*, 4358–4385. DOI: https://doi.org/10.1002/slct.201600693

[65] C. Nupearachchi, K. Mahatantila, M. Vithanage, *Groundwater Sustainable Develop.* **2017**, *5*, 206–215. DOI: https://doi.org/10.1016/j.gsd.2017.06.006
[66] J. Ma, D. Ping, X. Dong, *Membranes* **2017**, *7*, 52. DOI: https://doi.org/10.3390/membranes7030052
[67] *Graphene Oxide* (Eds: A. Dimiev, S. Eigler), Wiley, Chichester **2017**.
[68] C. Chua, M. Pumera, *Chem. Soc. Rev.* **2014**, *43*, 291–312. DOI: https://doi.org/10.1039/c3cs60303b
[69] Y. Cao, X. Li, *Adsorption* **2014**, *20*, 713–727. DOI: https://doi.org/10.1007/s10450-014-9615-y
[70] H. Zhu, Y. Xu, Y. Yan, J. Xu, C. Yang, *Langmuir* **2020**, *36*, 13613–13620. DOI: https://doi.org/10.1021/acs.langmuir.0c02450
[71] T. Liu et al., *Colloids Surf., B* **2012**, *90*, 197–203. DOI: https://doi.org/10.1016/j.colsurfb.2011.10.019
[72] W. Peng, H. Li, Y. Liu, S. Song, *J. Mol. Liq.* **2016**, *221*, 82–87. DOI: https://doi.org/10.1016/j.molliq.2016.05.074
[73] D. Cortés-Arriagada, A. Toro-Labbé, *Phys. Chem. Chem. Phys.* **2015**, *17*, 12056–12064. DOI: https://doi.org/10.1039/c5cp01313e
[74] Y. Shen, B. Chen, *Environ. Sci. Technol.* **2015**, *49*, 7364–7372. DOI: https://doi.org/10.1021/acs.est.5b01057
[75] J. Ma et al., *Environ. Sci. Technol.* **2017**, *51*, 2283–12292. DOI: https://doi.org/10.1021/acs.est.7b02227
[76] J. Zhang et al., *Langmuir* **2019**, *35*, 6861–6869. DOI: https://doi.org/10.1021/acs.langmuir.9b00589
[77] Z. Wang et al., *Environ. Pollut.* **2019**, *254*, 112854. DOI: https://doi.org/10.1016/j.envpol.2019.07.022
[78] Y. Zhou, C. Liang, J. Yu, X. Jiang, *J. Cent. South Univ.* **2019**, *26*, 813–823. DOI: https://doi.org/10.1007/s11771-019-4051-5
[79] M. Ghosh et al., *Langmuir* **2020**, *36*, 7400–7407. DOI: https://doi.org/10.1021/acs.langmuir.0c00924
[80] T. Yao, L. Qiao, K. Du, *Microporous Mesoporous Mater.* **2020**, *292*, 109716. DOI: https://doi.org/10.1016/j.micromeso.2019.109716
[81] A. Pandey, M. Deb, S. Tiwari, P. Pawar, S. Saxena, S. Shukla, *JOM* **2018**, *70*, 469–472. DOI: https://doi.org/10.1007/s11837-018-2765-8.A
[82] J. Luo, Z. Wang, H. Jiang, S. Liu, F. Xiong, J. Ma, *Langmuir* **2020**, *36*, 4637–4644. DOI: https://doi.org/10.1021/acs.langmuir.0c00297
[83] W. Wan et al., *Environ. Sci. Nano* **2016**, *3*, 107–113. DOI: https://doi.org/10.1039/c5en00125k
[84] L. Shi et al., *J. Am. Chem. Soc.* **2016**, *138*, 6360–6363. DOI: https://doi.org/10.1021/jacs.6b02262
[85] B. Hiew et al., *Process Saf. Environ. Prot.* **2018**, *116*, 262–286. DOI: https://doi.org/10.1016/j.psep.2018.02.010
[86] C. Zhang, Z. Chen, W. Guo, C. Zhu, Y. Zou, *Int. J. Biol. Macromol.* **2018**, *112*, 1048–1054. DOI: https://doi.org/10.1016/j.ijbiomac.2018.02.074
[87] K. Gupta, O. Khatri, *J. Colloid Interface Sci.* **2017**, *501*, 11–21. DOI: https://doi.org/10.1016/j.jcis.2017.04.035
[88] G. Zhao et al., *Dalton Trans.* **2011**, *40*, 10945–10952. DOI: https://doi.org/10.1039/c1dt11005e
[89] L. Lingamdinne, J. Koduru, Y. Choi, Y. Chang, J. Yang, *Hydrometallurgy* **2016**, *165*, 64–72. DOI: https://doi.org/10.1016/j.hydromet.2015.11.005
[90] D. Vilela, J. Parmar, Y. Zeng, Y. Zhao, S. Sánchez, *Nano Lett.* **2016**, *16*, 2860–2866. DOI: https://doi.org/10.1021/acs.nanolett.6b00768
[91] R. Sitko, M. Musielak, B. Zawisza, E. Talik, A. Gagor, *RSC Adv.* **2016**, *6*, 96595–96605. DOI: https://doi.org/10.1039/c6ra21432k
[92] S. Pourbeyram, *Ind. Eng. Chem. Res.* **2016**, *55*, 5608–5617. DOI: https://doi.org/10.1021/acs.iecr.6b00728
[93] R. DeFever, N. Geitner, P. Bhattacharya, F. Ding, P. Ke, S. Sarupria, *Environ Sci. Technol.* **2015**, *49*, 4490–4497. DOI: https://doi.org/10.1021/es505518r
[94] L. Cui et al., *Chem. Eng. J.* **2015**, *281*, 1–10. DOI: https://doi.org/10.1016/j.cej.2015.06.043
[95] N. Yousefi et al., *Nat. Nanotechol.* **2019**, *14*, 107–119. DOI: https://doi.org/10.1038/s41565-018-0325-6
[96] Y. You et al., *Carbon* **2018**, *129*, 415–419. DOI: https://doi.org/10.1016/j.carbon.2017.12.032
[97] S. Kumar, R. Nair, P. Pillai, S. Gupta, M. Iyengar, A. Sood, *ACS Appl. Mater. Interfaces* **2014**, *6*, 17426–17436. DOI: https://doi.org/10.1021/am504826q
[98] S. Akpotu, B. Moodley, *J. Environ. Manage.* **2018**, *209*, 205–215. DOI: https://doi.org/10.1016/j.jenvman.2017.12.037
[99] H. Ghafuri, M. Talebi, *Ind. Eng. Chem. Res.* **2016**, *55*, 2970–2982. DOI: https://doi.org/10.1021/acs.iecr.5b02250
[100] J. Huang, Z. Yan, *Langmuir* **2018**, *34*, 1890–1898. DOI: https://doi.org/10.1021/acs.langmuir.7b03866
[101] Y. Jiang et al., *Environ. Sci. Technol.* **2015**, *49*, 6846–6854. DOI: https://doi.org/10.1021/acs.est.5b00904
[102] Y. Yang, W. Wang, M. Li, H. Wang, M. Zhao, C. Wang, *Polym. Compos.* **2016**, *39*, 1663–1673. DOI: https://doi.org/10.1002/pc.24114
[103] H. Dai, Y. Huang, H. Huang, *Carbohydr. Polym.* **2018**, *185*, 1–11. DOI: https://doi.org/10.1016/j.carbpol.2017.12.073
[104] M. Mohseni Kafshgari, H. Tahermansouri, *Colloids Surf., B* **2017**, *160*, 671–681. DOI: https://doi.org/10.1016/j.colsurfb.2017.10.019
[105] C. Minitha, M. Lalitha, Y. Jeyachandran, L. Senthilkumar, R. Kumar, *Mater. Chem. Phys.* **2017**, *194*, 243–252. DOI: https://doi.org/10.1016/j.matchemphys.2017.03.048
[106] R. Sitko et al., *Dalton Trans.* **2013**, *42*, 5682–5689. DOI: https://doi.org/10.1039/c3dt33097d
[107] N. Mahmoodi, S. Maroofi, M. Mazarji, G. Nabi-Bidhendi, *J. Surfactants Deterg.* **2017**, *20*, 1085–1093. DOI: https://doi.org/10.1007/s11743-017-1985-1
[108] W. Cao, Y. Ma, W. Zhou, L. Guo, *Chem. Res. Chin. Univ.* **2015**, *31*, 508–513. DOI: https://doi.org/10.1007/s40242-015-4487-6
[109] A. Al Nafiey et al., *Chem. Eng. J.* **2017**, *322*, 375–384. DOI: https://doi.org/10.1016/j.cej.2017.04.039
[110] K. Zhang, H. Li, X. Xu, H. Yu, *Microporous Mesoporous Mater.* **2018**, *255*, 7–14. DOI: https://doi.org/10.1016/j.micromeso.2017.07.037
[111] L. Liu, L. Ding, X. Wu, F. Deng, R. Kang, X. Luo, *Ind. Eng. Chem. Res.* **2016**, *55*, 6845–6853. DOI: https://doi.org/10.1021/acs.iecr.6b01359
[112] Z. Chen et al., *J. Hazard. Mater.* **2016**, *310*, 188–198. DOI: https://doi.org/10.1016/j.jhazmat.2016.02.034
[113] Y. Wang et al., *J. Hazard. Mater.* **2018**, *344*, 849–856. DOI: https://doi.org/10.1016/j.jhazmat.2017.11.040

[114] J. Chen, B. Yuan, J. Shi, J. Yang, M. Fu, *Catal. Today* **2018**, *315*, 247–254. DOI: https://doi.org/10.1016/j.cattod.2018.02.044
[115] Y. Liu et al., *Chem. Eng. J.* **2018**, *336*, 263–277. DOI: https://doi.org/10.1016/j.cej.2017.12.043
[116] X. Chen, B. Chen, *Environ. Sci. Technol.* **2015**, *49*, 6181–6189. DOI: https://doi.org/10.1021/es5054946
[117] T. Ramakrishna et al., *Langmuir* **2020**, *36*, 13575–13582. DOI: https://doi.org/10.1021/acs.langmuir.0c02370
[118] J. Xiao, Y. Xie, H. Cao, Y. Wang, Z. Guo, Y. Chen, *Carbon* **2016**, *107*, 658–666. DOI: https://doi.org/10.1016/j.carbon.2016.06.066
[119] Y. Liu, N. Liu, Y. Han, X. Zhang, H. Huang, Y. Lifshitz, S. Lee, J. Zhong, Z. Kang, *Science* **2015**, *347 (6225)*, 970–974. DOI: https://doi.org/10.1126/science.aaa3145
[120] B. Zhu, P. Xia, W. Ho, J. Yu, *Appl. Surf Sci.* **2015**, *344*, 188–195. DOI: https://doi.org/10.1016/j.apsusc.2015.03.086
[121] L. Zhu, L. You, Y. Wang, Z. Shi, *Mater. Res. Express.* **2017**, *4*, 075606. DOI: https://doi.org/10.1088/2053-1591/aa7903
[122] J. Xu, Z. Wang, Y. Zhu, *ACS Appl. Mater. Interfaces* **2017**, *9*, 27727–27735. DOI: https://doi.org/10.1021/acsami.7b07657
[123] E. Haque, J. Jun, S. Talapaneni, A. Vinu, S. Jhung, *J. Mater. Chem.* **2010**, *20*, 10801–10803. DOI: https://doi.org/10.1039/c0jm02974b
[124] Y. Zhang et al., *ACS Nano.* **2016**, *10*, 9036–9043. DOI: https://doi.org/10.1021/acsnano.6b05488
[125] S. Kim, J. Oh, S. Park, Y. Shim, S. Park, *Chemistry* **2016**, *22*, 5142–5145. DOI: https://doi.org/10.1002/chem.201505100
[126] G. Dong, Z. Ai, L. Zhang, *RSC Adv.* **2014**, *4*, 5553–5560. DOI: https://doi.org/10.1039/c3ra46068a
[127] A. Mirzaei, Z. Chen, F. Haghighat, L. Yerushalmi, *Chemosphere.* **2018**, *205*, 463–474. DOI: https://doi.org/10.1016/j.chemosphere.2018.04.102
[128] L. Jiang et al., *ACS Sustainable Chem. Eng.* **2017**, *5*, 5831–5841. DOI: https://doi.org/10.1021/acssuschemeng.7b00559
[129] Y. Deng et al., *Appl. Catal., B* **2017**, *203*, 343–354. DOI: https://doi.org/10.1016/j.apcatb.2016.10.046
[130] J. Zhang, S. Fang, J. Mei, G. Zheng, X. Zheng, X. Guan, *Sep. Purif. Technol.* **2018**, *194*, 96–103. DOI: https://doi.org/10.1016/j.seppur.2017.11.035
[131] J. Mu, J. Li, X. Zhao, E. Yang, X. Zhao, *RSC Adv.* **2016**, *6*, 35568–35576. DOI: https://doi.org/10.1039/c6ra02911f
[132] S. Wong, N. Ngadi, I. Inuwa, O. Hassan, *J. Cleaner Prod.* **2018**, *175*, 361–375. DOI: https://doi.org/10.1016/j.jclepro.2017.12.059
[133] L. Dong, W. Liu, Y. Yu, L. Hou, P. Gu, G. Chen, *Sci. Total Environ.* **2019**, *647*, 1359–1367. DOI: https://doi.org/10.1016/j.scitotenv.2018.07.280
[134] A. Azimi, A. Azari, M. Rezakazemi, M. Ansarpour, *ChemBioEng. Rev.* **2017**, *4*, 37–59. DOI: https://doi.org/10.1002/cben.201600010
[135] H. Tounsadi, A. Khalidi, M. Abdennouri, N. Barka, *Desalin. Water Treat.* **2015**, *57*, 16633–16642. DOI: https://doi.org/10.1080/19443994.2015.1079739
[136] S. Kanchi, K. Bisetty, G. Kumar, M. Sabela, *Arab. J. Chem.* **2017**, *10*, S3084–S3096. DOI: https://doi.org/10.1016/j.arabjc.2013.11.050
[137] M. Bali, H. Tlili, *Int. J. Environ. Sci. Technol.* **2018**, *16*, 249–258. DOI: https://doi.org/10.1007/s13762-018-1663-5
[138] A. Macías-García, J. García-Sanz-Calcedo, J. Carrasco-Amador, R. Segura-Cruz, *Sustainability* **2019**, *11*, 2672. DOI: https://doi.org/10.3390/su11092672
[139] Q. Yu et al., *Sol. Energy* **2019**, *177*, 324–336. DOI: https://doi.org/10.1016/j.solener.2018.11.029
[140] A. Mukherjee, J. Okolie, A. Abdelrasoul, C. Niu, A. Dalai, *J. Environ Sci.* **2019**, *83*, 46–63. DOI: https://doi.org/10.1016/j.jes.2019.03.014
[141] Y. Zhao et al., *J. Hazard. Mater.* **2018**, *360*, 529–535. DOI: https://doi.org/10.1016/j.jhazmat.2018.08.039
[142] O. Ioannidou, A. Zabaniotou, *Renewable Sustainable Energy Rev.* **2007**, *11*, 1966–2005. DOI: https://doi.org/10.1016/j.rser.2006.03.013
[143] C. Moreno-Castilla, *Carbon* **2004**, *42*, 83–94. DOI: https://doi.org/10.1016/j.carbon.2003.09.022
[144] R. Baby, B. Saifullah, M. Hussein, *Nanoscale Res. Lett.* **2019**, *14*, 1–17. DOI: https://doi.org/10.1186/s11671-019-3167-8
[145] K. Foo, B. Hameed, *Adv. Colloid Interface Sci.* **2011**, *162*, 22–28. DOI: https://doi.org/10.1016/j.cis.2010.09.003
[146] N. Ando, Y. Matsui, R. Kurotobi, Y. Nakano, T. Matsushita, K. Ohno, *Water Res.* **2010**, *44*, 4127–4136. DOI: https://doi.org/10.1016/j.watres.2010.05.029
[147] J. Rivera-Utrilla, M. Sánchez-Polo, *Adsorption* **2011**, *17*, 611–620. DOI: https://doi.org/10.1007/s10450-011-9345-3
[148] S. Smith, D. Rodrigues, *Carbon* **2015**, *91*, 122–143. DOI: https://doi.org/10.1016/j.carbon.2015.04.043
[149] J. Perrich, *Activated Carbon Adsorption for Wastewater Treatment*, CRC Press, Boca Raton, FL **2018**.
[150] L. Paredes, C. Alfonsin, T. Allegue, F. Omil, M. Carballa, *Chem. Eng. J.* **2018**, *345*, 79–86. DOI: https://doi.org/10.1016/j.cej.2018.03.120
[151] E. Altıntıg, H. Altundag, M. Tuzen, A. Sarı, *Chem. Eng. Re.s Des.* **2017**, *122*, 151–163. DOI: https://doi.org/10.1016/j.cherd.2017.03.035
[152] M. Kobya, E. Demirbas, E. Senturk, M. Ince, *Bioresour. Technol.* **2005**, *96*, 1518–1521. DOI: https://doi.org/10.1016/j.biortech.2004.12.005
[153] Y. El Maguana, N. Elhadiri, M. Bouchdoug, M. Benchanaa, A. Jaouad, *Int. J. Chem. Eng.* **2019**, 8621951. DOI: https://doi.org/10.1155/2019/8621951
[154] A. Karumuri, D. Oswal, H. Hostetler, S. Mukhopadhyay, *Mater. Lett.* **2013**, *109*, 83–87. DOI: https://doi.org/10.1016/j.matlet.2013.07.021
[155] A. Bhatnagar, W. Hogland, M. Marques, M. Sillanpää, *Chem. Eng. J.* **2013**, *219*, 499–511. DOI: https://doi.org/10.1016/j.cej.2012.12.038
[156] J. Li et al., *Environ. Pollut.* **2018**, *234*, 677–683. DOI: https://doi.org/10.1016/j.envpol.2017.11.102
[157] F. Cao, C. Lian, J. Yu, H. Yang, S. Lin, *Bioresour. Technol.* **2019**, *276*, 211–218. DOI: https://doi.org/10.1016/j.biortech.2019.01.007
[158] Z. Sui, Q. Meng, X. Zhang, R. Ma, B. Cao, *J. Mater. Chem.* **2012**, *22*, 8767–8771. DOI: https://doi.org/10.1039/c2jm00055e
[159] Y. Han, Z. Xu, C. Gao, *Adv. Funct. Mater.* **2013**, *23*, 3693–3700. DOI: https://doi.org/10.1002/adfm.201202601
[160] K. Watson, M. Farré, N. Knight, *Sci. Total Environ.* **2016**, *542*, 672–684. DOI: https://doi.org/10.1016/j.scitotenv.2015.10.125

[161] S. Gonçalves, M. Strauss, F. Delite, Z. Clemente, V. Castro, D. Martinez, *Sci. Total Environ.* **2016**, *565*, 833–840. DOI: https://doi.org/10.1016/j.scitotenv.2016.03.041
[162] P. Biswas, R. Bandyopadhyaya, *Water Res.* **2016**, *100*, 105–115. DOI: https://doi.org/10.1016/j.watres.2016.04.048
[163] B. Reed, R. Vaughan, L. Jiang, *J. Environ. Eng.* **2000**, *126*, 869–873. DOI: https://doi.org/10.1061/(asce)0733-9372(2000)126:9(869)
[164] C. Galan, M. Silva, D. Mantovani, R. Bergamasco, M. Vieira, *Can. J. Chem. Eng.* **2018**, *96*, 2378–2386. DOI: https://doi.org/10.1002/cjce.23185
[165] Q. Wang et al., *RSC Adv.* **2018**, *8*, 14775–14786. DOI: https://doi.org/10.1039/c8ra00244d
[166] V. Suba, G. Rathika, E. Ranjith Kumar, M. Saravanabhavan, *J. Inorg. Organomet. Polym.* **2018**, *28*, 1706–1717. DOI: https://doi.org/10.1007/s10904-018-0831-x
[167] W. Qiu et al., *J. Alloys Compd.* **2016**, *678*, 179–184. DOI: https://doi.org/10.1016/j.jallcom.2016.03.304
[168] F. Mehrabi, A. Vafaei, M. Ghaedi, A. Ghaedi, E. Alipanahpour Dil, A. Asfaram, *Ultrason. Sonochem.* **2017**, *38*, 672–680. DOI: https://doi.org/10.1016/j.ultsonch.2016.08.012
[169] C. Han, M. Jing, X. Shen, G. Qiao, *J. Nanosci. Nanotechnol.* **2017**, *17*, 5327–5334. DOI: https://doi.org/10.1166/jnn.2017.13811
[170] H. Zhong, Y. Shaogui, J. Yongming, S. Cheng, *J. Environ. Sci.* **2009**, *21*, 268–272. DOI: https://doi.org/10.1016/S1001-0742(08)62262-7
[171] H. Bel Hadjltaief, A. Omri, M. Ben Zina, P. Da Costa, M. Galvez, *Adv. Mater. Sci. Eng.* **2015**, *2015*, 1–10. DOI: https://doi.org/10.1155/2015/759853
[172] T. Alslaibi, I. Abustan, M. Ahmad, A. Foul, *J. Chem. Technol. Biotechnol.* **2013**, *88*, 1183–1190. DOI: https://doi.org/10.1002/jctb.4028
[173] M. Noraini, E. Abdullah, R. Othman, N. Mubarak, *Mater. Lett.* **2016**, *184*, 315–319. DOI: https://doi.org/10.1016/j.matlet.2016.08.064
[174] A. Nayak, B. Bhushan, V. Gupta, P. Sharma, *J. Colloid Interface Sci.* **2017**, *493*, 228–240. DOI: https://doi.org/10.1016/j.jcis.2017.01.031
[175] M. Armandi, B. Bonelli, F. Geobaldo, E. Garrone, *Microporous Mesoporous Mater.* **2010**, *132*, 414–420. DOI: https://doi.org/10.1016/j.micromeso.2010.03.021
[176] C. Liang, Z. Li, S. Dai, *Angew. Chem. Int. Ed.* **2008**, *47*, 3696–3717. DOI: https://doi.org/10.1002/anie.200702046
[177] W. Yang, H. Chen, X. Han, S. Ding, Y. Shan, Y. Liu, *J. Hazard. Mater.* **2020**, *381*, 120981. DOI: https://doi.org/10.1016/j.jhazmat.2019.120981
[178] K. Gupta, D. Gupta, O. Khatri, *Appl. Surf. Sci.* **2019**, *476*, 647–657. DOI: https://doi.org/10.1016/j.apsusc.2019.01.138
[179] X. Cheng, A. Kan, M. Tomson, *J. Nanopart. Res.* **2005**, *7*, 555–567. DOI: https://doi.org/10.1007/s11051-005-5674-z
[180] V. Gupta, T. Saleh, *Environ. Sci. Pollut. Res.* **2013**, *20*, 2828–2843. DOI: https://doi.org/10.1007/s11356-013-1524-1
[181] V. Samonin, V. Nikonova, M. Podvyaznikov, *Russ. J. Appl. Chem.* **2014**, *87*, 190–193. DOI: https://doi.org/10.1134/s1070427214020116
[182] O. Alekseeva, N. Bagrovskaya, A. Noskov, *Prot. Met. Phys. Chem. Surf.* **2016**, *52*, 443–447. DOI: https://doi.org/10.1134/s2070205116030035
[183] H. Klefer, M. Munoz, A. Modrow, B. Böhringer, P. Wasserscheid, B. Etzold, *Chem. Eng. Technol.* **2016**, *39*, 276–284. DOI: https://doi.org/10.1002/ceat.201500445
[184] A. Romero-Anaya, M. Lillo-Ródenas, *Carbon* **2014**, *77*, 616–626. DOI: https://doi.org/10.1016/j.carbon.2014.05.066
[185] F. Lin, Y. Wang, Z. Lin, *RSC Adv.* **2016**, *6*, 33055–33062. DOI: https://doi.org/10.1039/c5ra27738h
[186] Q. Wu, W. Li, S. Liu, *Mater. Res. Bull.* **2014**, *60*, 516–523. DOI: https://doi.org/10.1016/j.materresbull.2014.09.015
[187] M. Liu et al., *Chin. Chem. Lett.* **2016**, *27*, 795–800. DOI: https://doi.org/10.1016/j.cclet.2016.01.038
[188] B. Chang, D. Guan, Y. Tian, Z. Yang, X. Dong, *J. Hazard. Mater.* **2013**, *262*, 256–264. DOI: https://doi.org/10.1016/j.jhazmat.2013.08.054
[189] S. Olivera et al., *Environ. Technol. Innovation* **2018**, *12*, 160–171. DOI: https://doi.org/10.1016/j.eti.2018.08.007
[190] K. Yang, J. Xing, P. Xu, J. Chang, Q. Zhang, K. Usman, *Polymers* **2020**, *12*, 236. DOI: https://doi.org/10.3390/polym12010236
[191] M. Sabet, K. Mahdavi, *Appl. Surf. Sci.* **2019**, *463*, 283–291. DOI: https://doi.org/10.1016/j.apsusc.2018.08.223
[192] P. Saud, B. Pant, A. Alam, Z. Ghouri, M. Park, H. Kim, *Ceram. Int.* **2015**, *41*, 11953–11959. DOI: https://doi.org/10.1016/j.ceramint.2015.06.007
[193] Y. Zhang, L. Wang, M. Yang, J. Wang, J. Shi, *Appl. Surf. Sci.* **2019**, *466*, 515–524. DOI: https://doi.org/10.1016/j.apsusc.2018.10.087
[194] Q. Wang, G. Wang, X. Liang, X. Dong, X. Zhang, *Appl. Surf. Sci.* **2019**, *467–468*, 320–327. DOI: https://doi.org/10.1016/j.apsusc.2018.10.165
[195] Z. Zhang et al., *Mater. Lett.* **2018**, *230*, 72–75. DOI: https://doi.org/10.1016/j.matlet.2018.07.086
[196] C. Liu et al., *Mater. Res. Bull.* **2020**, *122*, 110640. DOI: https://doi.org/10.1016/j.materresbull.2019.110640
[197] M. Mashkani, A. Mehdinia, A. Jabbari, Y. Bide, M. Nabid, *Food Chem.* **2018**, *239*, 1019–1026. DOI: https://doi.org/10.1016/j.foodchem.2017.07.042.M
[198] S. Huang et al., *Chem. Eng. J.* **2019**, *368*, 941–950. DOI: https://doi.org/10.1016/j.cej.2019.03.015
[199] S. Mallakpour, V. Behranvand, *J. Cleaner Prod.* **2018**, *190*, 525–537. DOI: https://doi.org/10.1016/j.jclepro.2018.04.120
[200] O. Rahmanian, M. Dinari, M. Abdolmaleki, *Appl. Surf. Sci.* **2018**, *428*, 272–279. DOI: https://doi.org/10.1016/j.apsusc.2017.09.152
[201] Y. Wu, T. Li, L. Yang, *Bioresour. Technol.* **2012**, *107*, 10–18. DOI: https://doi.org/10.1016/j.biortech.2011.12.088
[202] B. Arora, P. Attri, *J. Compos. Sci.* **2020**, *4*, 135. DOI: https://doi.org/10.3390/jcs4030135
[203] K. D. Pickering, in *Civil and Environmental Enginnering*, Rice University, Houstan, TX **2005**.
[204] O. V. Alekseeva, N. A. Bagrovskaya, A. V. Noskov, *Prot. Met. Phys. Chem. Surf.* **2016**, *52*, 443–447. DOI: https://doi.org/10.1134/S2070205116030035
[205] C. Moreno-Castilla, M. Alvarez-Merino, L. Pastrana-Martínez, M. López-Ramón, *J. Colloid Interface Sci.* **2010**, *345*, 461–466. DOI: https://doi.org/10.1016/j.jcis.2010.01.062
[206] S. Kurwadkar, T. V. Hoang, K. Malwade, S. R. Kanel, W. F. Harper Jr., G. Struckhoff, *Nanotechnol. Environ. Eng.* **2019**, *4*, 12. DOI: https://doi.org/10.1007/s41204-019-0059-1

[207] N. G. Khaligh, M. R. Johan, *NANO* **2018**, *13 (9)*, 1830006. DOI: https://doi.org/10.1142/S1793292018300062
[208] J. Xu, Z. Cao, Y. Zhang, Z. Yuan, Z. Lou, X. Xu, X. Wang, *Chemosphere* **2018**, *195*, 351–364. DOI: https://doi.org/10.1016/j.chemosphere.2017.12.061
[209] M. ben Mosbah, L. Mechi, R. Khiari, Y. Moussaoui, *Processes* **2020**, *8*, 1651. DOI: https://doi.org/10.3390/pr8121651
[210] P. S. Pamidimukkala, H. Soni, *J. Environ. Chem. Eng.* **2018**, *6*, 3135–3149. DOI: https://doi.org/10.1016/j.jece.2018.04.013
[211] S. Giraldo, I. Robles, A. Ramirez, E. Florez, N. Acelas, *SN Appl. Sci.* **2020**, *2*, 1029. DOI: https://doi.org/10.1007/s42452-020-2736-x
[212] S. Fan, J. Tang, Y. Wang, H. Li, H. Zhang, J. Tang, Z. Wang, X. Li, *J. Mol. Liq.* **2016**, *220*, 432–441. DOI: https://doi.org/10.1016/j.molliq.2016.04.107
[213] W. Q. Wu et al., *Water Air Soil Pollut.* **2013**, *224 (1)*, 1372. DOI: https://doi.org/10.1007/s11270-012-1372-5
[214] L. Dong, L. Hou, Z. Wang, P. Gu, G. Chen, R. Jiang, *J. Hazard Mater.* **2018**, *359*, 76–84. DOI: https://doi.org/10.1016/j.jhazmat.2018.07.030
[215] M. Yusuf, F. M. Elfghi, S. A. Zaidi, E. C. Abdullah, M. A. Khan, *RSC Adv.* **2015**, *5*, 50392–50420. DOI: https://doi.org/10.1039/C5RA07223A
[216] A. Hu, A. Apblett, *Lect. Notes Nanoscale Sci. Technol.* **2014**, 22.
[217] Y. Li et al., *Chem. Eng. Res. Des.* **2013**, *91*, 361–368. DOI: https://doi.org/10.1016/j.cherd.2012.07.007
[218] B. Cagnon, M. S. Secula, Ş. S. Bayazit, in *Carbon-Based Material for Environmental Protection and Remediation* (Eds: M. Bartoli, M. Frediani, L. Rosi), Intechopen, UK **2020**.
[219] M. N. Chong, B. Jin, C. W. K. Chow, C. Saint, *Water Res.* **2010**, *44*, 2997–3027. DOI: https://doi.org/10.1016/j.watres.2010.02.039
[220] R. C. Pawar, S. Kang, S. H. Ahn, C. S. Lee, *RSC Adv.* **2015**, *5*, 24281–24292. DOI: https://doi.org/10.1039/c4ra15560b
[221] M. Jani, J. A. Arcos-Pareja, M. Ni, *Molecules* **2020**, *25*, 4934. DOI: https://doi.org/10.3390/molecules25214934

The research progress made in recent years in the removal of heavy metal ions and organic-inorganic pollutants from wastewater by various carbon-based nanomaterials is reviewed and discussed. Nanosized and activated forms of carbonaceous nanomaterials with hierarchical structures proved to be more efficient in eliminating heavy metal ions and organic dyes as compared to routinely used adsorbents.

Carbon Nanomaterials for Wastewater Treatment

Hanna S. Abbo, K. C. Gupta*, Nader G. Khaligh, Salam J. J. Titinchi*

ChemBioEng Rev. **2021**, *8 (5)*, **XXX ··· XXX**

DOI: 10.1002/cben.202100003